NASA Technical Memorandum 107076
AIAA–95–2516

2.3 kW Ion Thruster Wear Test

Michael J. Patterson, Vincent K. Rawlin, and James S. Sovey
Lewis Research Center
Cleveland, Ohio

Michael J. Kussmaul and James Parkes
NYMA, Inc.
Brook Park, Ohio

Prepared for the
31st Joint Propulsion Conference and Exhibit
cosponsored by AIAA, ASME, SAE, and ASEE
San Diego, California, July 10–12, 1995

National Aeronautics and
Space Administration

2.3 kW Ion Thruster Wear Test

Michael J. Patterson*, Vincent K. Rawlin*, and James S. Sovey*
National Aeronautics and Space Administration
Lewis Research Center
Cleveland, Ohio

Michael J. Kussmaul and James Parkes
NYMA, Inc.
NASA Lewis Research Center Group
Brook Park, Ohio

A 30-cm diameter xenon ion thruster is under development at NASA to provide an ion propulsion option for auxiliary and primary propulsion on missions of national interest. Specific efforts include thruster design optimizations, component life testing and validation, and performance characterizations. Under this program, the ion thruster will be brought to engineering model development status. This paper describes the results of a 2.3-kW 2000-hour wear test performed to identify life limiting phenomena, measure the performance and characterize the operation of the thruster, and obtain wear, erosion, and surface contamination data. These data are being used as a data base for proceeding with additional life validation tests, and to provide input to flight thruster design requirements.

Introduction

Several flight experiments and demonstrations of ion propulsion are being conducted by the Europeans and Japanese during this decade.[1-3] In the United States, NASA has a program to develop ion thruster system technologies to satisfy auxiliary and primary propulsion requirements for missions of national interest. To date, a series of test programs has been conducted at NASA with laboratory version 30-cm ion thrusters and components to establish a database for development of an engineering model thruster. Goals of the engineering model thruster development effort include a thruster mass of ≤ 7 kg and an operating power envelope of 0.5 to 2.3 kW.

An engineering model xenon ion thruster is presently under development in the NASA Solar Electric Propulsion Technology Application Readiness (NSTAR) program established to validate ion propulsion for space flight applications. The fabrication of the first of several thrusters has been completed, and they incorporate innovations in design, materials, and fabrication techniques compared to those employed in conventional ion thrusters.

A 2000-hour wear test of the first engineering model ion thruster was conducted in a ground test facility that simulated the relevant space environment. The objectives of the test were to:

- demonstrate 2000 hours of continuous operation at a thruster input power of 2.3 kW and identify life limiting phenomena
- measure the performance and characterize the operation of the thruster
- obtain wear, erosion, and surface contamination data
- provide a data base for proceeding with additional

*Aerospace Engineer, Member AIAA

life validation tests and

- provide input to flight thruster design requirements.

This paper discusses the results of the 2000 hour wear test conducted at 2.3 kW input power on the engineering model thruster under development at NASA for the NSTAR program. This includes a detailed description of both the thruster and ground support equipment, and a discussion of pretest thruster documentation including both hardware documentation and thruster performance assessments. A discussion of the test results including the test chronology, test shutdowns, thruster performance over duration, and post test thruster analyses (hardware condition, documentation, and erosion measurements) are also presented.

Hardware Description

This section describes the experimental and ground support hardware used for the wear test.

Thruster

The engineering model thruster used in the wear test is shown in Figures 1a - 1d. This configuration is proposed for a flight application and it is being used to validate the design. This engineering model thruster, or EMT, was preceded by a functional model thruster, or FMT, that was used to define manufacturing processes and to verify the physical and functional design. Table 1 lists the design attributes of the EMT. The overall mass of the EMT, including 3 m cable harness, is approximately 6.4 kg and is somewhat lighter than the FMT.

The EMT was developed with certain operational and performance goals and objectives. These include: an input power envelope of 0.5 kW to 2.3 kW, with a service life of 12,000 h at full power; performance comparable to that demonstrated previously with the FMT and other 30 cm laboratory model thrusters;[4-10] design and interfaces that are compatible with the mission and system requirements for both auxiliary and primary propulsion applications; simplified power processing requirements; and reduced thruster size, mass (to approximately 7 kg), parts count, and fabrication costs.

The EMT, and the earlier FMT, incorporates innovations in design, materials, and fabrication techniques compared to those employed in conventional thrusters. These include a conic discharge chamber which transitions into a short cylindrical region immediately upstream of the ion optics. This partial-conic design is inherently more rigid and occupies less volume than conventional cylindrical shape thrusters, while still exhibiting good discharge characteristics and allowing for a uniform plasma distribution across the exit plane. Past development efforts have shown the large rear wall of cylindrical shape thrusters to be an inefficient stress-bearing structure and vulnerable to mechanical vibration.[11]

The use of non-ferromagnetic discharge chamber materials is a major departure from conventional ring-cusp thruster designs and previous thrusters. The engineering model thruster employs both 0.8 mm thick alloy 5052 aluminum and 0.5 mm thick AMS 4901 titanium for the discharge chamber, magnet retention rings, and other structural components. The use of aluminum and titanium, as opposed to steel, was motivated by a concern to minimize the thruster mass. This is because thruster mass reductions can create a 'ripple' effect that can significantly reduce the mass of a multi-thruster propulsion system.[12] An added advantage of aluminum is that the complex shape of the thruster can be readily fabricated using a spin forming technique at relatively low cost. Both die stamping and spin forming were originally considered as each technique permits seamless formation of complex shapes from a single sheet of metal. Because of its lower initial tooling cost, metal spinning is often preferred for low volume production and was used for fabricating the thruster aluminum components described herein.

The discharge hollow cathode did not employ a keeper or starting electrode and discharge-coupling to the anode was used for ignition and steady-state operation. The screen grid electrode was electrically isolated for this test. This was done in the expectation that the screen grid would float positive of cathode potential resulting in a reduction in the energy of the ions striking the screen grid and an increase in the life of the grid. All cathode potential surfaces in the discharge chamber, except the hollow cathode assembly itself, are eliminated in the thruster design. This approach reduces the total number of components subjected to sputtering via discharge plasma ions to an absolute minimum.

The thruster uses a distributed 'reverse-injection' propellant manifold for the discharge chamber flow, where the propellant is introduced into the discharge chamber near the ion optics and directed backwards toward the cathode. The reverse-feed approach has been shown in previous laboratory experiments to improve the propellant efficiency obtainable especially at throttled conditions, as compared to the conventional approach of introducing the propellant at the rear of the discharge chamber.

The EMT is designed to accommodate a simplified power processing approach. The thruster is normally operated using four commercial power supplies for steady-state operation, with two additional power supplies required for cathode conditioning. A total of seven power leads to the thruster are required. In a flight system, the power processor will consist of a total of four power supplies to operate the thruster (both for start-up and steady-state operation). This reduction in power processing requirements is implemented by combining functions performed by multiple power supplies into single custom modules, with the benefit of reduced parts count and mass.[13]

A ring-cusp magnetic circuit is employed in the thruster.[7] This design uses high-field strength, rare-earth permanent magnets in rings of alternating polarity along the perimeter of the chamber, with the field lines terminating on anode potential surfaces. Three cusps are located in the discharge, one each in the regions of the discharge cathode, the discharge sidewall (at the conic-cylinder intersection), and the ion optics-end.

The discharge chamber and neutralizer cathode assemblies for the EMT consist of a hollow cathode assembly composed of a high temperature refractory alloy tube and an S-type impregnated insert. Both assemblies also use a sheathed heater design, derived from the mercury ion thruster, used for both activation and ignition of the cathodes.[11] The neutralizer cathode assembly incorporates an enclosed-keeper electrode design to improve gas efficiency, with critical design parameters established to maximize ion transparency and reduce beam-coupling potentials. Overall mass of the neutralizer assembly and its titanium mounting bracket is approximately 250 grams.

Two-grid design ion optics were used for the EMT. This design was derived from an engineering model mercury ion thruster.[11] The electrodes are fabricated from molybdenum and are dished outward. The electrodes are attached to thicker molybdenum stiffening rings, which are in turn attached to a titanium ring to form the ion optics assembly. The accelerator ring is electrically isolated from the titanium mounting ring with 12 equally spaced insulators. The titanium ring is in turn electrically isolated from the anode-potential discharge chamber via six equally space insulators. The mass of the EMT ion optics are approximately 1.88 kg.

The EMT screen electrode thickness is 0.51 mm, while the accelerator electrode is 0.38 mm. The screen grid thickness was increased from that on the FMT to permit reduced accelerator grid operating voltages and increased grid lifetime. The apertures are of circular shape, with inner circle diameters of 1.91 mm and 1.14 for the screen and accelerator grids, respectively. The open-area-fractions are 0.67 and 0.22 for the screen and accelerator grid, respectively. The nominal cold grid gap is set at 0.66 mm. The screen grid hole pattern dimensions were reduced from those of the accelerator grid to reduce beam divergence losses. The electrode geometries are listed in Table 2.

At the time of the wear test, an engineering model low-pressure propellant isolator design had not been adopted. For the conduct of the wear test, laboratory-class service isolators were used. For high voltage isolation, a fluoro-elastomer tube of approximately 1 m length was used for the main plenum flow, while a series of 10 cryogenic breaks, enclosed within a plasma screen, were used for the discharge cathode flow. A single shadow-shielded cryogenic break was used for low-voltage isolation of the neutralizer propellant flow.

The plasma screen of the EMT is fabricated from 0.25 mm thick 304 stainless steel. It is constructed of 3 separate pieces which are seam welded together to form a single unit. The stainless steel is chemically-etched to an open-area-fraction of about 50% with 0.51 mm diameter holes over about 80% of it's total surface, and it has a total mass of about 590 grams.

Ground Support Equipment

Laboratory power supplies were used for the thruster wear test.[4] The EMT uses four laboratory power supplies for steady-state operation (discharge, beam, accelerator, and neutralizer keeper), with two additional power supplies for the start-up of discharge and neutralizer cathodes. As discussed above, the screen grid of the thruster was electrically isolated from discharge cathode-common, and permitted to float.

All tests were performed using high-purity xenon propellant. The propellant feed system used was constructed using an all-electropolished stainless-steel tubing construction consisting of welds and metal-gasket seals. The three feed lines to the thruster (main, cathode, and neutralizer) incorporated individual commercial mass flow controllers to measure the propellant flow rate. Each controller was calibrated using instrumentation traceable to a primary standard.

Post-test calibrations of the propellant feed system mass flow controllers were not conducted until a considerable

time had elapsed, during which period the flow controllers had been cycled on and off. While the post-test calibrations for the discharge cathode and neutralizer cathode controllers were, within the measurement uncertainty, essentially identical to the pre-test calibrations, the main plenum flow controller calibration indicated a considerable shift. At the wear test main plenum flow rate, the post-test calibration indicated a 7.5% reduction in flow rate; that is, there is the possibility that the flow rate at the end of the wear test was in actuality as much as 7.5% lower than indicated from the pre-test calibration. This would mean that the performance values presented herein are conservative.

As no flow-rate calibrations were conducted immediately after the conduct of the wear test, corrections to the data for this phenomenon are problematic, and therefore the data are presented corrected solely using pre-test calibrations. It is noted here however that a reduction in the main plenum flow rate may have occurred over the conduct of the wear test, which could have also exacerbated the observed erosion.

The thruster wear test was conducted in NASA's large space simulation testbed. The chamber is 4.6 m in diameter by 19.2 m in length. For the wear test, a pumping speed of approximately 340 kℓ/s xenon pumping speed was achieved using a combination of twenty 0.9 m diameter oil diffusion pumps and a 27 m^2 cryopanel. The no-load pressure was $\leq 3.3 \times 10^{-5}$ Pa, with an operational pressure (thruster at 2.3 kW) of about 2.0×10^{-4} Pa.

The thruster was operated open-loop; that is, no closed-loop control on any thruster parameters. The data were recorded via a computer data acquisition system from calibrated digital metering. Additionally, two eight-channel strip-chart recorders were used for continuous monitoring of thruster and power-supply parameters. Two independent control systems, one associated with the power supplies, and one with the computer acquisition system, were implemented to permit steady state, unattended operation of the thruster. In the event of thruster or facility parameters out-of-range of pre-specified values, the thruster would be commanded off.

All thruster performance data were corrected for thrust losses associated with beam divergence and doubly-charged ions. Total efficiency and specific impulse calculations included losses associated with accelerator drain and neutralizer power, and neutralizer flow rate. All propellant efficiencies included a correction to the mass flow rate for propellant ingested from the facility. A detailed discussion of the thruster performance calculations can be found in reference 10.

Pretest Thruster Documentation

Hardware

Pre-wear test documentation of the thruster components was conducted to allow comparisons with their post-test condition. Documentation of the ion optics included measurements of hole geometries and diameters on both grids, thickness measurements of both grids at multiple locations, precision mass measurements of both grids, assembled grid-gap measurements, and photography of both grids at multiple locations. Pretest documentation of both discharge and neutralizer cathodes included measurements of orifice plate dimensions, and photography of the orifice plates and tubes. Discharge chamber documentation included magnetic field measurements at the magnet surfaces, anode surfaces, and in the discharge volume.

Prior to final assembly and documentation of the thruster, all major components underwent an ultrasonic cleaning process. Final thruster assembly was conducted using clean-room procedures. Prior to installation of the thruster in the vacuum chamber, leakage resistance across thruster high-voltage surfaces and insulators was measured using a high voltage ohmmeter.

Performance

Immediately after final assembly of the thruster and prior to initiation of the wear test, tests were conducted to characterize the thruster performance. These data included discharge current-voltage characteristics obtained at 2.3 kW, neutralizer keeper and coupling voltages versus neutralizer propellant flow rate, and accelerator grid impingement current versus total accelerating voltage. These data are compared to data obtained directly after the wear test.

Test Results

Chronology

Table III lists the sequence of events and anomalies which occurred during the conduct of the wear test. During the first portion of the test, to approximately 867 elapsed hours, there were several interruptions to examine thruster power-throttling performance as well as to understand the magnitude and AC-component of the observed accelerator grid impingement current.

The most notable anomaly was a test interruption that occurred at approximately hour 867. An initial failure of the logic which controlled the sequencing of the high voltage power supplies during arcing resulted in a thruster

shutdown. Before this failure was identified, repeated attempts were made to restart the thruster and extract an ion beam. During this process, without the arc protection afforded by the high voltage control logic, the thruster and service propellant isolators were stressed to at least 3000 volts potential. This caused a mechanical failure of the discharge cathode service propellant isolators and resulted in a propellant leak. This propellant leak precluded restarting the thruster once repairs to the power supply control logic were effected.

The failure of the service propellant isolators required that the vacuum chamber be vented to atmosphere to repair the thruster. On examination of the thruster, additional damage to the discharge cathode assembly was identified. This damage was evident as erosion of downstream face of the discharge cathode heater coil surrounding the cathode orifice plate. At that time, the damage was suspected to be caused by electron-backstreaming during the failed restart attempts at hour 867, and the cathode was replaced by an identical unit. Subsequently it was identified that the erosion was a consequence of sputtering by discharge ions (discussed later).

After replacement of the damaged service propellant isolators and the discharge cathode assembly, and after erosion measurements of the ion optics were obtained, the thruster was reassembled and testing was resumed. The remaining portion of the wear test, which was voluntarily terminated after approximately 2031 hours of operation at 2.3 kW, was interrupted sporadically due to failures of the neutralizer power supply and high voltage power supplies. None of these events, however, compromised the condition of the thruster.

Thruster Performance

Table IV summarizes the thruster nominal (time-average) operating and performance parameters over the 2031 hours of the wear test using the original pre-test flow calibration. The data were obtained from the data acquisition and control system, and reduced in the manner described in Ref. 10. As indicated, the average test conditions were 2300 W input power at approximately 3310 seconds specific impulse and 65 percent overall thruster efficiency, providing a thrust of approximately 92 mN. As discussed above, the post test calibration showed a 7.5% reduction in main flow with no change in neutralizer or cathode flow which would make these average test values conservative.

Figures 2 and 3 respectively, show the overall thruster efficiency and specific impulse versus time for the 2031 hour wear test duration. As indicated in Fig. 2, the thruster experienced an overall efficiency decay of approximately 5%; approximately 3% from hour 0 to 186, and 2% from hour 186 to 2031. At hour 186, after throttling performance data were obtained, the discharge (cathode emission) current was increased from 11.8 A to 12.2 A which increased the discharge propellant efficiency from a low of about 88% back to a value of about 93%. Additionally, the neutralizer propellant flow rate was trimmed from an initial value of about 3.4 sccm to 2.9 sccm to improve thruster efficiency.

A corresponding reduction in specific impulse is observed in Fig. 3, going from approximately 3300 seconds down to 3150 seconds. The decrease in both the thruster efficiency and specific impulse correlate reasonably well with the decrease in total propellant efficiency over the test duration; or more precisely, the reduction in beam current for fixed-flow operation. This magnitude of efficiency decay, approximately 2-3% per thousand hours of operation for open-loop fixed-flow operation, is consistent with that previously observed in the 5.5 kW wear test.[4]

The large vertical bandwidth for the efficiencies and specific impulse values in Figs. 2 and 3 is due to the rather large variation in output voltage of the screen power supply; approximately ± 50 volts.

Figure 4 and 5 respectively, show the thruster input power and thrust for the wear test duration. The thruster input power initially decayed from about 2300 W to 2150 W over the first 187 hours, corresponding to a drop in beam current. Subsequently, the input power remained at about 2300-2350 W. The thrust also dropped over the first 187 hours, from about 93 mN to 88 mN, and subsequently stayed within about ± 3 mN of 92 mN for the remaining portion of the test.

discharge chamber and cathode - The discharge losses over the wear test averaged about 183 W/A electrical, at a discharge chamber propellant efficiency of about 91%, corrected for propellant ingestion and estimated doubly-charged ions. The discharge losses, after adjustment of the discharge current at hour 186, varied by about ± 11 W/A, while the propellant efficiency varied by about ± 2%. These variations reflect changes in the beam current and the discharge voltage.

Minor variations in discharge voltage were experienced over the wear test duration. At hour 186 when the discharge cathode emission current was increased, a step-function change in the discharge voltage occurred, from

about 25 V to 26.5 V. From hour 186 until hour 867 the discharge voltage remained fairly constant, within approximately ± 0.25 V. At the hour 867 shutdown, the discharge cathode assembly was replaced, and the test was resumed. A gradual increase in discharge voltage was subsequently experienced to approximately 27.5 V at about hour 1600, at which point the voltage remained fairly constant for the remainder of the wear test. This long-term variation in discharge voltage, for tests under which the cathode is operated at fixed emission current and flow rate conditions, is typical of that experienced in other long-duration hollow cathode wear tests.[14,15] Variations of as much as ± 2 V are observed, and are believed to be due to the natural evolution of the emitter surface condition, and not associated with any deleterious reactions attributable to cathode contamination.

ion optics - Figures 6 and 7 show the high-voltage recycle rate, and cumulative number of recycles, for the wear test duration. It is noteworthy that only 14 recycles were experienced during the first 867 hours of operation. Subsequent to removal of the thruster at hour 867 for repairs, the recycle rate increased dramatically, accumulating an additional 379 recycles for the remainder of the test. This rate increase is at least in part due to the spalling of deposited thin-films on the ion optics; the spalling effected by high-humidity atmospheric exposure of the thruster. A maximum recycle frequency of 37 in 24 hours was experienced subsequent to the restart of thruster after failure of the screen power supply at hour 1495. Subsequently the recycle rate averaged about 5 per 24 hours for the remainder of the wear test.

Prior to restarting the thruster on hour 867, and subsequent restarts of the thruster, grid-to-grid, and on occasion screen grid-to-engine body, shorts were identified during leakage resistance measurement tests. The shorting, presumably due to thin-film flakes, were cleared upon the application of high voltage.

Figure 8 shows the ratio of the accelerator grid impingement current-to-beam current, as a percentage, versus wear test duration. The ratio started at 0.55% and decreased to about 0.47% by the end of the test. Noteworthy are two large transients; one during the first few hundred hours of operation, and the second subsequent to the restart of the test at hour 867. These long-term rises in accelerator current after hour 187 and hour 867 are contrary to prior experience, and are as of yet unexplained. It is noted that the peak-to-peak AC component of the accelerator current was equal in magnitude to the DC component, and is has been hypothesized that these phenomena may be related.[16]

neutralizer - The neutralizer cathode performed nominally throughout the duration of the wear test. At hour 187, the neutralizer flow rate was trimmed from 3.4 sccm to 2.9 sccm to improve overall thruster efficiency. There were, during the second portion of the wear test, a few occasions of neutralizer extinction resulting from power supply failure. The neutralizer was subsequently restarted after each extinction without incident. Figure 9 shows the neutralizer keeper and coupling voltages over the duration of the wear test. The average values of the keeper and coupling voltages were 12.7 V and -10.9 V, respectively. As indicated in Fig. 9, both voltages exhibited a decrease in about 1 V magnitude over the first 400 hours of operation. After exposure of the thruster to atmosphere at hour 867, both voltages restarted at approximately their initial values and decayed again by about 1 V over the subsequent 400 hours and then remained fairly constant for the remainder of the test.

ground support equipment - As noted in Table III, there were several instances during the conduct of the wear test when failures of the high voltage power supplies occurred. In most cases these were associated with failure of the output voltage regulation stage. In addition, the neutralizer keeper power supply was damaged and replaced on occasion. It is believed to have been damaged during a high-voltage arc transient when neutralizer-common potential was driven substantially negative of facility-ground. Problems with the computer data acquisition system also resulted in loss of test data, from about hour 695 to 717, from about hour 1216 to 1236, and from hour 1874 to 1887.

Post Test Thruster Analyses

Performance

Subsequent to the completion of the wear test and prior to removal of the thruster from the vacuum chamber, a variety of performance assessments were conducted on the thruster. These included conducting a performance sensitivity-analysis about the nominal 2.3 kW condition, obtaining power-throttling data, and examining the operation of the ion optics and neutralizer.

The sensitivity of the discharge voltage and beam current to variations in cathode emission current was examined at the end of the wear test. Both the discharge voltage and beam current varied linearly over a range of emission currents from about 10.0 A to about 12.5 A. At the end of the test, however, the discharge voltage at a given emission current was approximately 1 volt higher than

that measured prior to the start of the wear test. Similarly, the beam current was approximately 100 mA lower, for a given emission current and indicated flow rate, at the end of the test as compared to that measured at the start of the test.

Power-throttling data were obtained for the thruster during the conduct of the test at hour 21, hour 187, and at the end of the wear test at hour 2031. Table V compares the thruster performance, at the nominal wear test condition (operating point 1), for these run hours. Note that the thruster efficiency decayed from about 65.1% at run hour 21 down to 62.2% at the end of the test, all data obtained at the same input flow rate. Note that this was due to a decrease in input power as a consequence of a reduction in beam current (the reduction in beam current due to a thruster performance decay, or possibly flow drift). The flight power processor unit will contain an algorithm to maintain constant beam current via adjustment of the discharge current, a feature not implemented in the wear test. For the last 1840 hours of the test, at approximately a constant input power, the thruster efficiency only dropped by about 0.8%. From hour 187, to the completion of the test, the thruster efficiency decreased by about 1.4% at operating point 2. For operating points 3-6 (at run hour 21), the thruster efficiency dropped from between 1.9% and 2.4%; while for points 7-10 (at run hour 187), the efficiency dropped from between 0.8% and 2.3%. Note that these performance numbers are based on the pretest calibrations. Using post-test flow controller calibration data yields higher thruster performance values and/or lower efficiency decays.

Using an impingement current rate-of-rise of 0.1 mA/V as a definition of the 'knee' of the curve of screen potential versus beam current, the perveance (minimum total voltage) at full power varied non-linearly with time over the conduct of the test, from about 860 volts to 925 volts. During the wear test, the base-level impingement current varied from about 8.2 mA a few hours from the start of the test to approximately 8.4 mA at the end of the test. The accelerator grid holes enlarged with no apparent impact on perveance. The electron-backstreaming limit measured prior to the start of the wear test, and upon the completion of the wear test at hour 2031, was unchanged and approximately -145 volts accelerator grid potential at the nominal 2.3 kW condition.

The neutralizer mass flow rate was varied about the nominal run flow at run hour 187, and again at the end wear test to measure the sensitivities of the keeper voltage and coupling voltage at full-power. The keeper voltage data are shown in Fig. 10, and they indicate that there was essentially no change in the function of the neutralizer as a consequence of the wear test.

Hardware

After the wear test, a thorough examination of the thruster was performed, and a preliminary analysis of the results obtained from the thruster hardware has been completed. After removal from the vacuum chamber, the analysis began with a complete visual inspection and photodocumentation of the ion thruster. Leakage resistance measurements and physical measurements were made at this time. Major components of the thruster were removed (ion optics, plasma screen, and neutralizer and discharge cathode assemblies) and were prepared for further close-up photography, measurement, and disassembly.

Deposition samples (spalled flakes and spalling films) were removed from discharge chamber surfaces, and magnetic field mapping of the discharge were performed. Scanning electron microscopy (SEM) micrographs were taken of the discharge deposition samples to estimate film thicknesses, and x-ray microanalysis (Energy Dispersive Analysis by X-rays, or EDAX) was performed on the samples to determined the elemental composition of the films. The neutralizer cathode assembly, and both discharge cathode assemblies used during the wear test were photographed, and measurements were made of the orifice plate geometries.

A preliminary examination of the thruster components while still on the test stand indicated that several had survived the wear test with little or no damage. These undamaged components included most thruster structural elements and insulators, the neutralizer cathode, and all wiring. Components which had experienced damage included minor erosion of the neutralizer keeper due to interception by beam-ions, and charge-exchange erosion of the downstream surface of the accelerator grid. Additionally, severe erosion of the downstream surface of the discharge cathode orifice plate and heater (as observed during the first portion of the wear test) was evident. During subsequent disassembly, severe erosion of the upstream surface of the screen electrode, and spalling of deposited films on discharge surfaces in close-vicinity to the screen electrode, became evident.

Results obtained from analyses of the major thruster components include:

discharge chamber - Within the measurement uncertainty there was no change in discharge magnetic field; that is, no discernable irreversible losses due to thermal degradation.

As noted previously, there was significant deposition and spalling of thin films. The spalling films were confined to the most-forward interior portion of the discharge chamber on the titanium anode surface and along the interior lip of the forward magnet retention ring, and also along the main plenum electropolished tube and the stainless steel plenum support clips. All these surfaces are within 2 cm of the downstream end of the discharge chamber and in close-proximity to the screen electrode. All other discharge chamber surfaces upstream of this region were free of spalled films, and no flakes or particles could be removed from these surfaces by abrasive contact. Examination of the thruster discharge chamber at hour 867 had identified some spalling from the main plenum and plenum support clips, but none was evident from the titanium anode surface itself.

EDAX analysis of flakes from both the most-forward anode surface (the lip of the magnetic retention ring), and the main plenum tube indicated that the main elemental composition was molybdenum (from the screen electrode), with only traces of tantalum (from the discharge cathode).

The flake from the anode surface had a clear interface region through it's thickness, likely associated with exposure of the thruster to air after the initial 867 hour test segment. About 2.0 microns of molybdenum were deposited during the first test segment. A 4.7 micron film was deposited during the course of the remaining 1164 hours of the wear test. The average deposition rate during the 867 hour segment was approximately 2.3 μm/khr and the rate for the second segment was 4.0 μm/khr, yielding a 74% increase in rate. Similar measurements of a flake obtained in nearly the same location gave rates of 2.8 μm/khr and 4.0 μm/khr, for an increase in rate of 43%.

Assuming a uniform deposition of a 6.7 micron film at the magnet retainer lip (which is at 14.0 cm radius) from a 15.2 cm diameter disk in the center of the screen grid, this would result in a disk mass loss of about 2.5 grams. This is consistent with the mass loss of the screen grid, which was about 4.0 grams.

discharge cathode assembly - The discharge cathode orifice and chamfer on both cathode assemblies (the original plus the replacement at hour 867) completed their respective test segments in virtually pristine condition with no depositions and no change in diameters. However the outer radius of the orifice plates, in the region of the plate/tube electron beam weld joint, as well as the downstream face of the cathode heater coil, experienced severe erosion. See Figures 11a and 11b, before and after photographs from the 867-hour-segment discharge cathode.

The erosion of the orifice plate was severe enough to remove the entire electron beam weld seam (which was originally about 130 microns above the surface of the plate) from the downstream surface of the orifice plate. The average depth erosion measured at the outer-most radius of molybdenum-alloy edge of the first-segment cathode (which operated for about 867 hours) was about 250 microns. Approximately 250 microns inside the edge the erosion depth (into the thoriated-tungsten plate) averaged about 110 microns. For the second-segment discharge cathode, which operated for about 1164 hours plus an additional 100 hours of diagnostic testing, an edge-erosion depth of 330 microns was measured. Approximately 250 microns inside the edge the erosion depth was approximately 210 microns. The magnitude of the erosion, assuming a linear process with time, is unacceptable as the original orifice plate thickness is of the order of 1240 microns.

Those portions of the helical cathode heater coil (approximately 270 degrees of it's downstream face) which originally protruded downstream of the cathode orifice plate by a maximum of about 640 microns, were completely eroded away. The pattern of erosion implied a point source of high-energy ions very close to the cathode orifice expanding radially outward. The erosion resulted in complete removal of the downstream surface of the tantalum outer sheath of the swaged heater for about 30 degrees and 45 degrees of the most-forward coil on the first- and second-segment discharge cathodes respectively. In both cases this resulted in exposure of the ceramic insulator surrounding the center conductor. Despite the severe erosion, neither heater exhibited any degradation in performance.

The tantalum radiation shielding covering the exterior axial portions of the heater sheath on the second-segment cathode experienced significant erosion. The radiation shielding consists of approximately twelve layers of wrapped tantalum, each layer about 13 microns thick, covering approximately all of the 2.2 cm axial length of the heater. On the second-segment cathode, the first layer

of shielding was completely eroded away over approximately the first centimeter of it's length starting from the tip of the cathode. On the first-segment cathode, the erosion of the radiation shielding was much less severe, indicating an increase in the cathode erosion rate during the second portion of the wear test.

The deposited film on the main cathode insulator, a small portion of which is exposed to the discharge, was analyzed and was found to be primarily composed of rhenium, molybdenum and tantalum, with a trace of iron and aluminum. This composition implies some ion erosion of the cathode tube. This is consistent with the 'frosted' appearance of the tube upstream of the heater, although measurements of the tube diameter indicated a negligible degree of wall-thinning occurring.

A boroscopic examination of the electron-emitting impregnated insert was performed on both discharge cathodes. This visual examination did not reveal any anomalous material transport or material formation which would be indicative of life-limiting reactions due to exposure to reactive contaminants.

ion optics - Based on pre- and post-test measurements, there was no change in the assembled grid-to-grid cold-gap or alignment for the wear test within the measurement uncertainty.

The screen grid experienced unexpectedly high, severe, erosion resulting in a significant reduction in the thickness of the grid. Combined optical and direct measurements of the grid on axis indicated a thickness reduction of approximately 100 μm $\pm$ 10 μm at the minimum-thickness location, which was along a line joining 2 screen holes. Note that pretest thickness measurements of the screen grid were not made in order to preclude the possibility of damaging the grid. Similarly fabricated screen grids, however, have a thickness of 363 μm $\pm$ 3 μm. The reduction in screen grid thickness was due to a combination of a uniform electrode thinning (about 83 μm), as well as chamfering around the upstream perimeters of the screen grid holes in the center of the grid (about 43 μm maximum, but about 17 μm in the region of uniform thinning).

The thickness reduction in the center of the screen grid corresponds to an erosion rate of approximately 46 μm/khr (the grids accumulated approximately 2150 hours of total operation, including additional development tests subsequent to the completion of the wear test and prior to examination). Assuming the erosion rate is constant with time, at this rate the screen grid would be completely worn through in 7.8 khr. This erosion rate is inconsistent with the requirements of the life validation program which includes a 12-khr test at full power. The overall screen grid mass loss was 4.040 grams $\pm$ 0.001 grams. These results are summarized in Table VI. Figures 12a-12c show the upstream center of the screen grid at hour 0, hour 867, and hour 2150, respectively.

After the first portion of the wear test, the thruster was removed from the vacuum chamber which permitted examination and quantification of the charge-exchange erosion on the downstream surface of the accelerator grid. For the first 867 hours, the average bridge-erosion depth (the region of minimum erosion between the charge-exchange pits) around the center holes of the grid was measured to be 12 microns $\pm$ 5 microns. This measured value compares favorably to the value predicted using a simple grid erosion parameter,[17] which yields 13 μm. After the conclusion of the wear test, these measurements were repeated and indicated an average bridge-erosion depth of 20 μm $\pm$ 5 μm. This value is somewhat lower than the 31 μm predicted using the grid erosion parameter. At this erosion rate, the accelerator grid would be eroded to 40% of it's original thickness (a conservative estimate of end-of-life) within 21,500 hours. The results of the accelerator grid examinations, including the magnitude of the pit erosion, are summarized in Table VII. The accelerator grid suffered a mass loss of 1.965 grams $\pm$ 0.001 grams over the conduct of the wear test. Figures 13a-13c show the charge-exchange erosion on the downstream center of the accelerator grid at hour 0, hour 867, and hour 2150, respectively.

The accelerator grid holes, out to approximately half-radius, enlarged by approximately 0.10 mm, from an initial diameter of about 1.14 mm. Beyond half-radius, the hole-enlargement dropped off linearly with radius, to zero enlargement at full-beam radius. The open area of the grid increased by about 11% over the duration of the test, from approximately 0.222 to 0.246.

neutralizer assembly - As was the case for the discharge cathode, the neutralizer cathode orifice and chamfer, and the impregnated insert completed the test in virtually pristine condition. Unlike the discharge cathode, however the neutralizer cathode experienced virtually no erosion of the orifice plate, or electron-beam weld seam on the downstream face of the orifice plate, or cathode heater sheath.

The only anomalous condition identified with the neutral-

izer assembly was minor erosion of the exterior surface of the keeper tube. This erosion, due to direct ion interception of the keeper via energetic high angle beam ions, was concentrated on the tip of the assembly on the beam-facing side, over the first 1.3 cm of it's length. Based on tube wall thickness measurements at the tip of the keeper, the worst-case erosion was about 17.8 μm/khr. Assuming a constant wear-rate, in 12-khr hours the worst-case erosion of the keeper tube would be about 216 μm out of an overall thickness of about 500 μm.

Discussion

The results from the post-test examination of the thruster are summarized in Table VIII. The following conclusions may be drawn from an interpretation and analysis of the results obtained from the post-test examination of the thruster components:

The screen grid erosion was unacceptably high. The most likely explanation for the excessive screen grid erosion rate is that it was caused by the screen grid floating several volts negative of cathode potential. During the wear test the screen grid was intentionally allowed to float electrically in the expectation that the screen grid would float positive of cathode potential, and hence reduce the energy of the ions striking the screen grid and increase it's life.

A previous 900 hour wear test of a ring-cusp ion thruster operating on xenon at 5.5 kW, however, indicated that screen grid erosion was insignificant when the discharge voltage was maintained at $\leq$ 28 volts with the screen grid tied electrically to cathode potential.[4] The EM thruster wear test was conducted at a comparable discharge voltage, and at half the total power level of the 900 hour test, suggesting that the screen grid erosion, with the grid at cathode potential, should not be a problem.

No measurements of the screen grid floating potential were made during the wear test. The thruster was reassembled and retested after the wear test. The results of these tests indicated that the screen grid floating potential could be several volts below cathode potential, and that the floating potential is a strong function of the discharge chamber propellant efficiency. Screen grid floating potentials in the range of 33.0-33.7 volts (with respect to anode potential) were measured over the nominal propellant efficiency range.

Screen grid erosion estimates were made based on centerline doubly-to-singly charged ion measurements that were obtained after the conduct of the wear test. With the screen grid floating, a 30% ratio was obtained on centerline, at the wear test condition. Assuming a beam flatness parameter of 0.5, an ion flux of 0.30 A to the screen electrode, and a floating potential of 33.4 V, a centerline erosion of 105 μm is estimated. This compares favorably to the 100 μm $\pm$ 10 μm measured.

Subsequent measurements in a different facility with the screen grid tied to cathode-common potential indicated a centerline ratio of approximately 13% at the wear test condition.[18] At this screen potential (26.8 V) and doubly-charged ion ratio, a screen erosion rate of about 8.8 μm/khr is estimated. This would yield a screen grid lifetime of 20,700 h, where end-of-life is erosion on centerline to half of it's original thickness. Based on these analyses, it would appear that the screen grid erosion observed during the wear test could be accounted for by its large floating potential, and the measured doubly-to-singly charged ions on centerline.

Accelerator grid erosion by charge-exchange ions does not appear to be a factor in thruster wear out lifetime at 2.3 kW. At the observed erosion rates, the accelerator grid end-of-life is substantially greater than the required 12-khr service life. This conclusion holds even if the post-test flow calibration data were used for the entire test duration. That is, readjustment of the thruster propellant efficiency to account for the potential of a calibration shift would yield, at maximum, a 35% increase in the impingement current (to about 11.3 mA), and correspondingly, a 35% increase in erosion rate, reducing the lifetime to about 16,000 h.

The spalling of sputter-deposited material in the discharge chamber was sufficient after 867 hours of operation to result in repeated inter-grid, and screen grid to engine body shorting after the thruster had been exposed to atmosphere. The sputter-deposited films of molybdenum were up to 6.7 μm thick, and were poorly adhering to the stainless steel and titanium surfaces on the forward end of the discharge chamber. It is clear, since the sputter-deposited films are molybdenum, that the source of the material was the screen electrode. Reducing the screen grid erosion by changing it's potential will reduce the material deposition rate. Note that after 867 hours of operation, the 2.0 μm films deposited were spalling. Even if the erosion of the screen grid were reduced by an order-of-magnitude, it is possible that spalling may occur prior to the required 12-khr thruster service life if a sputter containment system were not implemented.

Significant erosion to the orifice plates of both discharge cathodes used in the wear test occurred. In both cases, the orifice plate to cathode tube weld on the downstream edge of the plate was completely eroded away. Cathode failure could occur if the orifice plate is eroded completely through. A re-examination of the orifice plate from the 900 hour thruster wear test at 5.5 kW[4] suggests that it too likely suffered this type of erosion. The observed damage is believed to result from the bombardment of energetic ions produced by the operation of the hollow cathode.

The observed cathode heater damage to the downstream sheath surface is believed to be due to the same erosion mechanism which eroded the cathode orifice plate. Sufficient erosion of the heater sheath could cause an open circuit in the heater resulting in heater failure and the inability to start the discharge cathode. The observed erosion damage to the heater in this wear test is inconsistent with the heater from the 5.5 kW test[4] which showed no evidence of damage. It is also inconsistent with the wear test of four hollow cathodes conducted in support of the space station plasma contactor program.[15]

In all the of the cathode tests where no heater erosion was observed, the downstream end of the heaters were positioned approximately 1.7 mm upstream of the cathode orifice plate. In these cases, the cathode orifice plates shielded the heaters from the energetic ions produced by the cathodes. For this wear test, however, the heater was positioned approximately 0.64-.76 mm downstream of the end of the cathode orifice plate, exposing it to the energetic ions. Clearly the erosion of the discharge cathode orifice plate and heater is unacceptable and necessitates a redesign.

The erosion rate of the neutralizer keeper assembly due to energetic beam ions appears to be low. Any possibility of penetration of the keeper housing, however, could be eliminated by the addition of a low sputter coefficient material.

Thruster Modifications

Erosion Mitigation

To mitigate the screen grid erosion, the grid will be electrically tied to cathode potential. Based on estimated erosion rates using the measured doubly-charged ion current fraction, and based on prior thruster wear tests, this should be sufficient to eliminate screen grid erosion as a factor in thruster wear out lifetime. If this is insufficient to extend the thruster service life, lowering the discharge propellant efficiency to reduce the doubly-charged ion fraction, lowering the discharge voltage, and/or adding nitrogen to the propellant could be done to further reduce grid erosion.

To preclude spalling of deposited films in the discharge chamber, a sputter containment system will be implemented. This system includes the application of grit-blasted stainless steel mesh to the forward end of the discharge chamber on all titanium and stainless steel surfaces. Additionally, all other discharge chamber surfaces will be grit-blasted. Grit-blasting both the mesh and rearward discharge surfaces to achieve ≈ 10 μm surface features should provide adequate flake control, for flakes up to 30 μm size.[19]

Several modifications to the discharge cathode assembly will be implemented to mitigate erosion. The electron-beam weld joining the orifice plate and tube will be repositioned from the forward surface of the plate to the side of the cathode tube to preclude direct ion erosion. The heater will be repositioned to a location approximately 1.7 mm behind the plane of the cathode tip. Additionally, the discharge cathode will be enclosed within a keeper assembly to protect the cathode orifice plate, heater, and radiation shield from ion sputtering. The discharge cathode keeper will be tied to anode potential through a high-impedance (nominally 1 kOhm).

Ground Support Equipment

There is supporting evidence, based on erosion rates, that the main plenum mass flow controller did shift during the conduct of the wear test. These data include: the unexpectedly high ratio of doubly-to-singly charged ion current measured at the end of the wear test (possibly due to a higher-than-anticipated propellant utilization efficiency); the apparent increase in erosion rate of the screen grid during the second-half of the wear test as indicated by the optical measurements at hour 867 and hour 2031, and the relative thicknesses of the sputter deposited films in the discharge chamber; the linear shift in the discharge voltage versus cathode emission current from beginning to end of the test which could have occurred by a change in main plenum flow rate of the order of the calibration shift; and temporal variations in the discharge voltage and beam current over the conduct of the wear test which may be indicative of changes in the main plenum flow rate. In order to prevent future occurrences of flow rate measurement problems, it is recommended that future long-duration wear tests use independent means of in-situ calibration of the individual propellant flow rates to the thruster to identify possible long-term calibration shifts which may occur and this has been implemented.

Performance Augmentation

To mitigate the performance degradation experienced over the conduct of the wear test, especially at deeply-throttled conditions, it would be advantageous to improve the thruster efficiency. Significant performance gains may be realized, especially in the 500-1000 W range, by redesign of the neutralizer to reduce its xenon flow rate and power consumption. Figure 14 shows the thruster efficiency loss, due to neutralizer operation, for the conditions identified in Table V. At 2.3 kW, the neutralizer reduces the thruster efficiency by about 8-10 percentage points, and at 0.5 kW it reduces the thruster efficiency by 20 percentage points.

An approach to developing a low flow, low power-consumption neutralizer design is to reduce the neutralizer cathode orifice, and concurrently, reduce the keeper current. The former insures proper spot mode operation at low flows, while the latter permits a reduction in neutralizer flow rate.

Note that the required neutralizer flow rate is to first-order directly proportional to the total neutralizer emission current (the sum of the keeper current and beam current).[20] From this, it is clear why significant performance gains could not be realized with the present neutralizer design. This is because the keeper current was 2.0 A, operating over a beam current range of approximately 1.8 A at 2.3 kW to 0.5 A at 0.5 kW. This represents a total range of emission current of 1.5:1.0 (from 3.8 A down to 2.5 A). For a fixed neutralizer flow rate over the power-throttling range, one could not reduce the flow below about 3.0 sccm to accommodate the 3.8 A of emission required at 2.3 kW (which is equivalent to 32% of the flow into the thruster at 0.5 kW), or for a variable flow approach, one could not throttle the neutralizer flow rate by more than about 1.5:1.0. Based on these considerations, a neutralizer redesign effort is on-going.

Conclusions

An engineering model xenon ion thruster is presently under development at NASA to provide an ion propulsion option for missions of national interest. A 2000-hour wear test of the first engineering model ion thruster was conducted in a ground test facility that simulated the relevant space environment to obtain long-term performance and wear data and to validate the technology readiness for space flight applications. The objectives of the test included demonstrating 2000 hours of continuous operation at a thruster input power of 2.3 kW identifying life limiting phenomena, and providing input to the flight thruster design.

A total of 2031 hours were accumulated at 2.3 kW input power. The average thruster wear test conditions were 2300 W input power at approximately 3310 seconds specific impulse and 65 percent overall thruster efficiency, providing a thrust of approximately 92 mN, based on pre-test calibrations of the propellant feed system. The thruster experienced an overall efficiency decay of approximately 5%; approximately 3% from hour 0 to 186, and 2% from hour 186 to 2031, which is consistent with the efficiency decay observed on prior wear tests for open-loop fixed-flow thruster operation.

Post-test calibrations of the propellant feed system mass flow controllers indicate the possibility of a flow drift during the conduct of the wear test. This would mean that the thruster performance at the end of the test may have been higher than indicated, due to a higher than anticipated propellant efficiency, and this could have been a major contributor to the observed grid wear. It is recommended that future long-duration wear tests use independent means of in-situ calibration of the individual propellant flow rates to the thruster to identify possible long-term calibration shifts.

After the wear test, a thorough examination of the thruster was performed, and results obtained from analyses of the major thruster components include: The screen grid experienced unexpectedly high, severe, erosion resulting in a significant reduction in the thickness of the grid. The most likely explanation for the excessive screen grid erosion rate is that it was caused by the screen grid floating several volts negative of cathode potential, and possibly a high doubly-to-singly charged ion concentration. Measurements with the screen grid tied to cathode-common potential indicated a screen erosion rate of about 8.8 μm/khr would be expected. This would yield a screen grid lifetime of 20,700 h, where end-of-life is erosion on centerline to half of it's original thickness.

There was significant deposition and spalling of thin films in the discharge chamber. The spalling films were confined to the most-forward interior portion of the discharge chamber. To preclude spalling of deposited films in the discharge chamber, a sputter containment system will be implemented. Additionally, the discharge cathode orifice plates, as well as the downstream face of the cathode heater coil, experienced severe erosion. The observed damage is believed to result from the bombardment of energetic ions produced by the operation of the

hollow cathode. Several modifications to the discharge cathode assembly are being implemented to mitigate erosion, including enclosing the discharge cathode within a keeper assembly to protect the cathode orifice plate, heater, and radiation shield from ion sputtering.

Accelerator grid erosion by charge-exchange ions does not appear to be a factor in thruster wear out lifetime at 2.3 kW. At the observed erosion rates, the accelerator grid end-of-life is substantially greater than the required 12-khr service life.

Acknowledgements

The authors would like to express their appreciation to Eli Green, George Jacynycz, Craig Nelson, Eugene Pleban, and Robert Roman for test support and thruster assembly. Also the support of Vince Scullin and George Soulas in development of the data acquisition and control system is gratefully acknowledged.

References

[1]Groh, K., et. al., "Development Status of the RIT Ion Engines, " AIAA Paper No. 90-2671, July 1990.

[2]Fearn, D.G., "The Proposed Demonstration of the UK-10 Ion Propulsion System on ESA's SAT-2 Spacecraft," IEPC Paper No. 88-031, October 1988.

[3]Kajiwara, K. and Katada, M., "Test Facilities for the ETS-VI Ion Engine System," AIAA Paper No. 90-2656, July 1990.

[4]Patterson, M.J. and Verhey, T.R., "5kW Xenon Ion Thruster Lifetest," AIAA Paper No., 90-2543, July 1990.

[5]Rawlin, V.K., "Internal Erosion Rates of a 10-kW Xenon Ion Thruster," AIAA Paper No. 88-2192, July 1988.

[6]Patterson, M.J. and Rawlin, V.K., "Performance of 10-kW Class Xenon Ion Thrusters," AIAA Paper No. 88-2914, July 1988.

[7]Sovey, J.S., "Improved Ion Containment Using a Ring-Cusp Ion Thruster," *Journal of Spacecraft and Rockets*, Vol. 21, Sept.-Oct. 1984, pp. 488-495.

[8]Rawlin, V.K., "Characterization of Ion Accelerating Systems on NASA's Ion Thrusters," AIAA Paper No. 92-3827, July 1992.

[9]Patterson, M.J., "Low-Isp Derated Ion Thruster Operation," AIAA Paper No. 92-3203, July 1992.

[10]Patterson, M.J., Haag, T.W., and Hovan, S.A., "Performance of the NASA 30 cm Ion Thruster," IEPC Paper No. 93-108, September 1993. (Also NASA TM-1064226).

[11]30-Centimeter Ion Thruster Subsystem Design Manual," NASA TM-79191, June 1979.

[12]Rawlin, V.K. and Majcher, G., "Mass Comparisons of Electric Propulsion Systems for NSSK of Geosynchronous Spacecraft," AIAA Paper No. 91-2347, June 1991.

[13]Rawlin, V.K., Pinero, L., and Hamley, J., "Simplified Power Processing for Inert Gas Ion Thrusters," AIAA Paper No. 93-2397, June 1993.

[14]Sarver-Verhey, T.R., "Continuing Life Test of a Xenon Hollow Cathode for a Space Plasma Contactor," AIAA Paper No. 94-3312, June 1994.

[15]Soulas, G.C., "Multiple Hollow Cathode Wear Testing for the Space Station Plasma Contactor," AIAA Paper No. 94-3310, June 1994.

[16]Kaufman, H.R, personal communication, January 1995.

[17]Patterson, M.J., Haag, T.W., Rawlin, V.K., and Kussmaul, M.T., "NASA 30 cm Ion Thruster Development Status," AIAA Paper No. 94-2849, June 1994. (Also NASA TM-106842).

[18]Myers, R.M., Pencil, E.J., Rawlin, V.K., Kussmaul, M., and Oden, K., "NSTAR Ion Thruster Plume Impacts Assessments," AIAA Paper No. 95-2825, July 1995.

19Power, J.L. and Hiznay, D.J., "Solutions for Discharge Chamber Sputtering and Anode Deposit Spalling in Small Mercury Ion Thrusters," NASA TM X-71675, March 1975.

[20]Patterson, M.J. and Mohajeri, K., "Neutralizer Optimization," IEPC Paper No. 91-151, October 1991.

Table I - EM Thruster Design Attributes

Attribute	EM Thruster
Mass, kg	6.4
Structural Material	Al 5052 and Ti AMS 4901
Assembly Fasteners	blind rivets
Propellant Isolators	cryogenic-breaks used for high voltage isolation (low-pressure isolators under development)

Table II EM Thruster Ion Optics Electrode Design

electrode design	electrodes	
attribute	screen	accelerator
electrode thickness, mm	0.36	0.51
hole diameter, mm	1.91	1.14
open-area-fraction	0.67	≈ 0.22

Table III - Wear Test Events

Elapsed Time, hours	Event/Anomaly
0.0	test start, 1705 h, 06.23.94
21.5 - 23.0	throttling data obtained
40.2	power interruption and thruster shutdown, 0915 h, 06.25.94: restart at 1110 h
92.2	thruster shutdown via operator error, 1515 h, 06.27.94: restart at 1845 h
105.5 - 105.6	tank press. to 10^{-4} torr & HV commanded off for 13 minutes: HV back on 0817 h, 06.28.94
158.4 - 158.8	He cryopanel high temperature and facility pressure increase: recovered at 1340 h, 06.30.94
183.9 - 185.5	throttling data obtained: new 2.3 kW condition established at 1613 h, 07.01.94, after ion optics check
282.3	neut. com.-to- neut. kpr. discharge extinguished 3 times via operator error, during attempts to examine Ja on oscilloscope
523.7 - 524.2	thruster taken off-line for perveance check: back on-line at 1755 h, 07.15.94
537.6 - 537.7	thruster taken off-line to check Ja vs. Jb, by varying Jd at fixed Vt
591.1	thruster taken off-line to check Ja, shutdown, restarted: off-line at 1351 h, wear test restart at 1530 h
658.3 - 661.1	thruster taken off-line to check Ja, HV on & off: back to run condition at 1330 h, 07.21.94
682.8 - 683.4	thruster taken off-line to check Ja, HV on & off: back to run condition at 1150 h, 07.22.94
754.4	cryopanel problems, and corresponding high facility pressure and Ja
824.3 - 827.5	ODP Quadrants off sequentially to check Ja, and perveance check: back on-line at 1159 h, 07.28.94
847.5 - 851.7	Xe bled into facility via external source to check Ja
866.9	thruster shutdown on low Jb due to high voltage power supply control failure, 0330h, 07.29.94: GSE failures and operator error on restart attempt at 0630 h, 07.29.94
866.9	wear test restart - 09.16.94 new discharge cathode assembly, and replacement service high-voltage isolators
874.8 - 875.5	high voltage off for repair of screen power supply
1308.9 - 1310.0	neutralizer off due to keeper power supply failure
1495.3	thruster shutdown due to screen power supply failure
1536.4 - 1537.8	neutralizer off due to keeper power supply failure: high voltage off from hour 1537.6 - 1537.8
1819.4	thruster shutdown due to accelerator power supply failure
1832.5	thruster shutdown due to Helium cryopanel failure
2030.8	wear test voluntarily terminated 0730 h, 11.04.94

Table IV - Nominal Wear Test Conditions

Parameter	Value
Overall Thruster Efficiency, %	65
Specific Impulse, s	3310
Thrust, mN	92
Input Power, W	2300
Discharge Propellant Efficiency, %	91.1
Total Propellant Efficiency, %	81.9
Discharge Losses, W/A	183
Screen Voltage, V	1106
Accelerator Grid Voltage, V	-183
Discharge Voltage, V	26.8
Neutralizer Keeper Voltage, V	12.7
Neutralizer Coupling Voltage, V	-10.9
Beam Current, A	1.76
Accelerator Grid Impingement Current, mA	8.40
Discharge Current, A	12.1
Neutralizer Keeper Current, A	2.0
Main Plenum Propellant Flow Rate, sccm	22.9
Discharge Cathode Propellant Flow Rate, sccm	2.97
Neutralizer Cathode Propellant Flow Rate, sccm	2.91
Total Operating Time @ 2.3 kW	≈ 2030 hours
Total High-Voltage Arcs during Test	393

Table V - Power-Throttling Data Obtained during Wear Test

Run Hour	Input Power, W	Specific Impulse, s	Thrust, mN	Efficiency, %	Mass Flow Rate, mg/s	Operating Point
21	2260	3260	92	65	2.89	1
187	2180	3140	89	63	2.89	1
2031	2190	3130	89	62	2.88	1
187	2330	3380	94	67	2.84	2
2031	2330	3340	93	65	2.84	2
21	1890	3480	70	63	2.05	3
2031	1820	3350	67	61	2.05	3
21	1360	3240	49	57	1.56	4
2031	1360	3170	48	55	1.56	4
21	780	3050	28	53	0.92	5
2031	810	3030	27	51	0.92	5
21	520	2250	20	44	0.92	6
2031	510	2120	20	41	0.97	6
187	2190	3290	89	66	2.76	7
2031	2200	3280	89	65	2.76	7
187	2250	3490	89	68	2.60	8
2031	2180	3380	86	65	2.60	8
187	1690	3440	65	65	1.93	9
2031	1660	3370	64	63	1.93	9
187	1200	3210	45	60	1.43	10
2031	1220	3200	45	58	1.43	10

Table VI - Screen Grid Erosion, Upstream Center

Elapsed Time, hours	Electrode Thinning, μm, $\pm$ 5 μm	Chamfering, μm, $\pm$ 5 μm	Maximum Erosion, μm, $\pm$ 10 μm	Time to Wear to Half-Thickness
867	-	$\approx$ 10	-	-
2150	83	48	100 μm[a]	3,900 h

[a]The thinning and chamfering do not occur at the same location. The minimum electrode thickness on centerline occurs where chamfers of 2 adjacent holes overlap resulting in a maximum erosion of about 100 μm.

Table VII - Accelerator Grid Maximum Charge-Exchange Erosion, Downstream Center

Elapsed Time, hours	Pit Erosion, μm, $\pm$ 10 μm	Bridge Erosion, μm, $\pm$ μm	Time to Wear:	
			through electrode at pits	through 40% of electrode at bridge (EOL)
867	31	12	14,300 h	14,400 h
2150	66	20	16,600 h	21,500 h

Table VIII - Wear Test Anomalies and Associated Thruster Modifications

Anomaly	Thruster Modification
Excessive Erosion of Screen Grid	Tie Screen Grid to Cathode-Common
Spalling of Sputter Deposited Material in Discharge	Add Sputter Containment Mesh
Erosion of Discharge Cathode Orifice Plate	• Relocate Weld Joint • Add Enclosed Keeper
Erosion of Discharge Cathode Heater	• Relocate Heater Upstream • Add Enclosed Keeper
Erosion of Discharge Cathode Radiation Shield	Add Enclosed Keeper
Direct Impingement on Neutralizer Assembly	Add Low-Sputter Yield Shield to Keeper

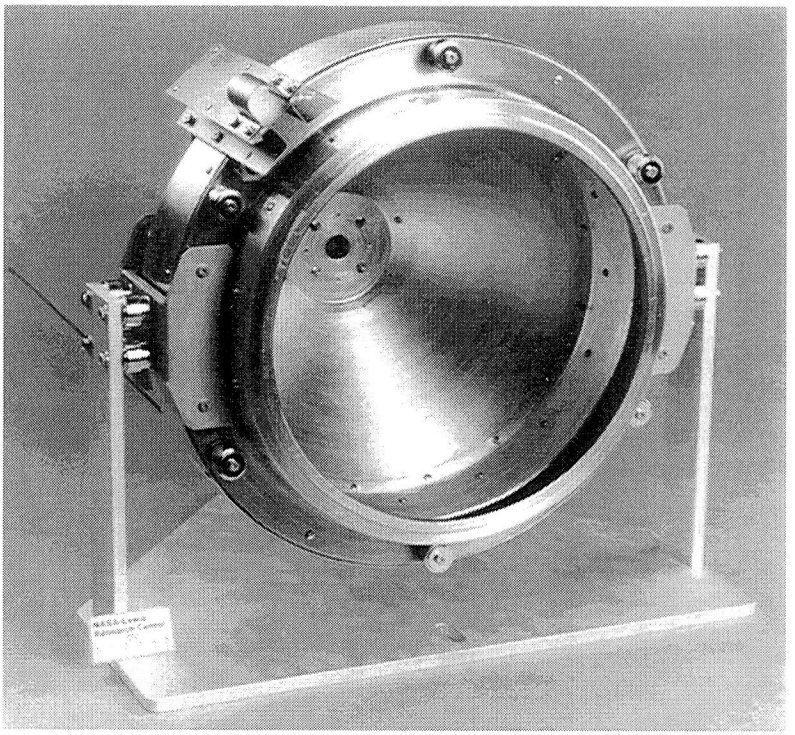

Figure 1a - Wear test thruster, less discharge and neutralizer cathode assemblies, ion optics, and plasma screen.

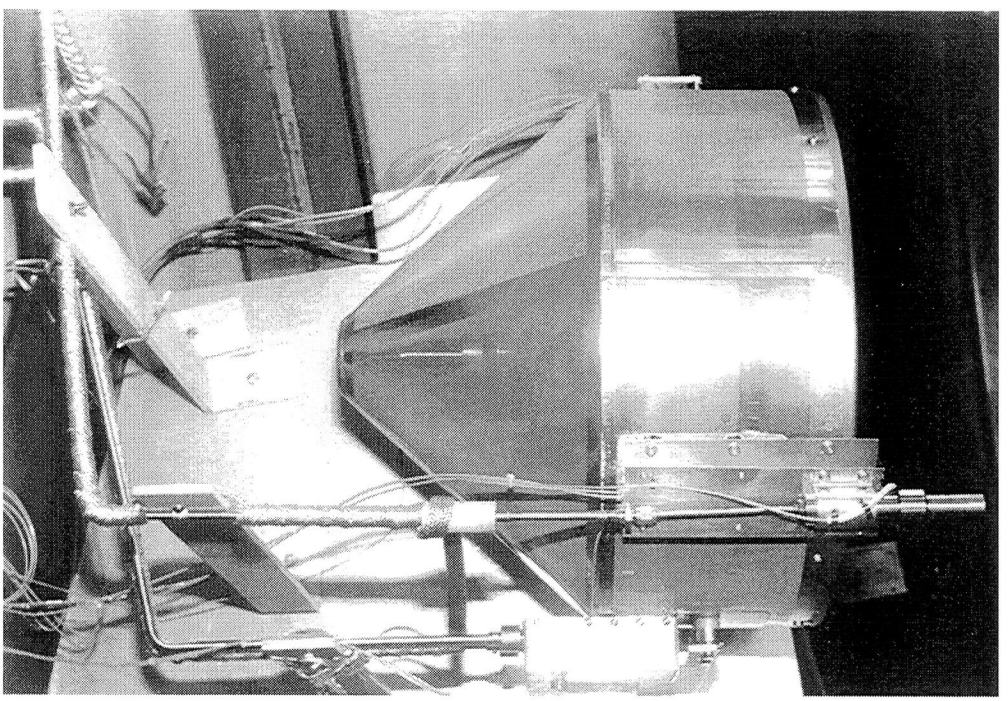

Figure 1b - Wear test thruster on test stand.

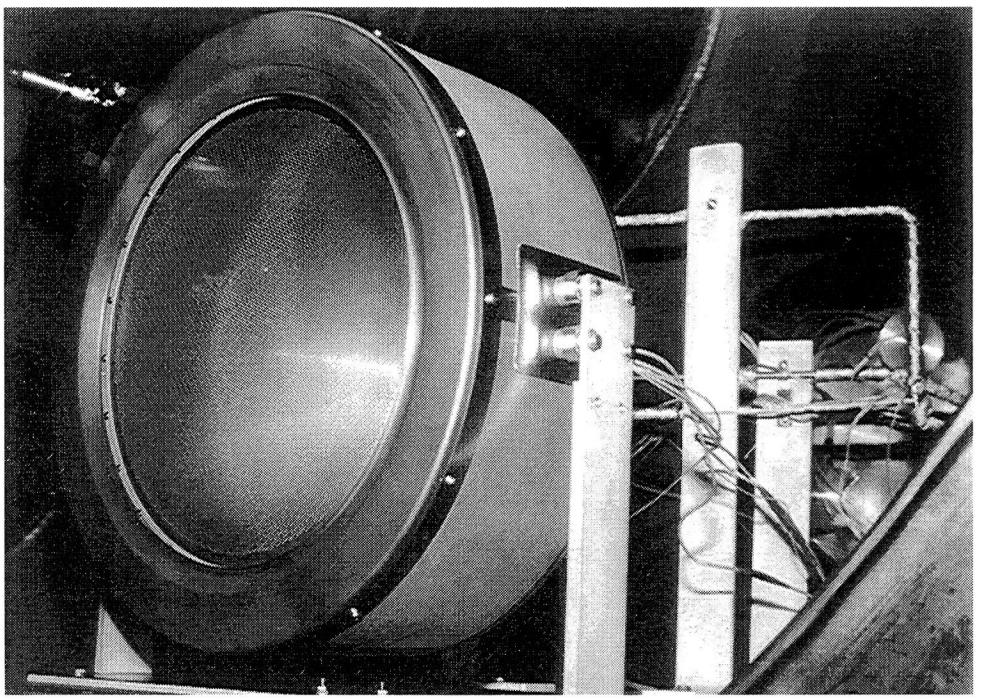

Figure 1c - Wear test thruster on test stand.

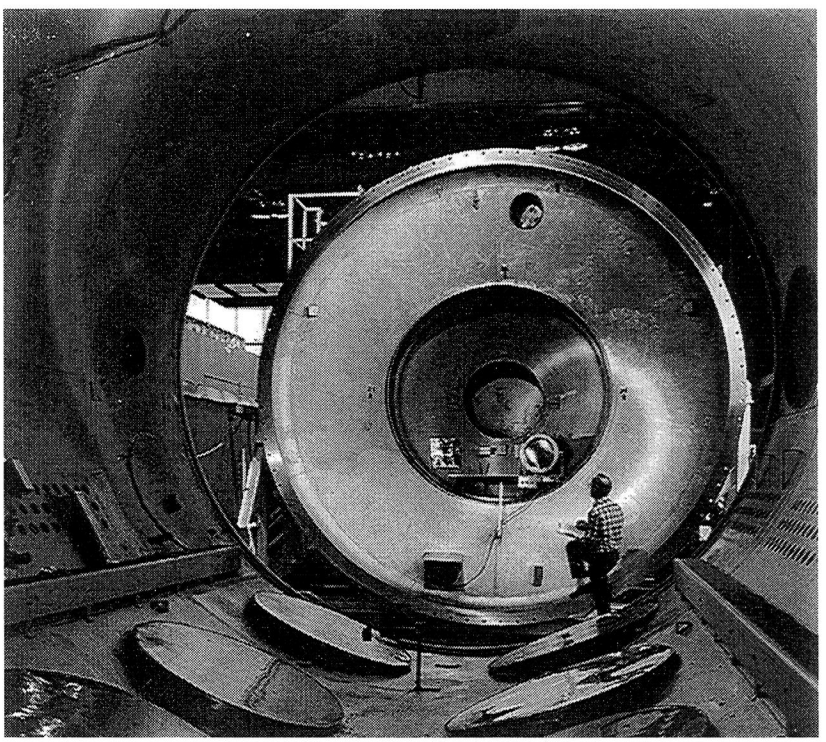

Figure 1d - Wear test thruster on test stand; vacuum facility endcap rolled back.

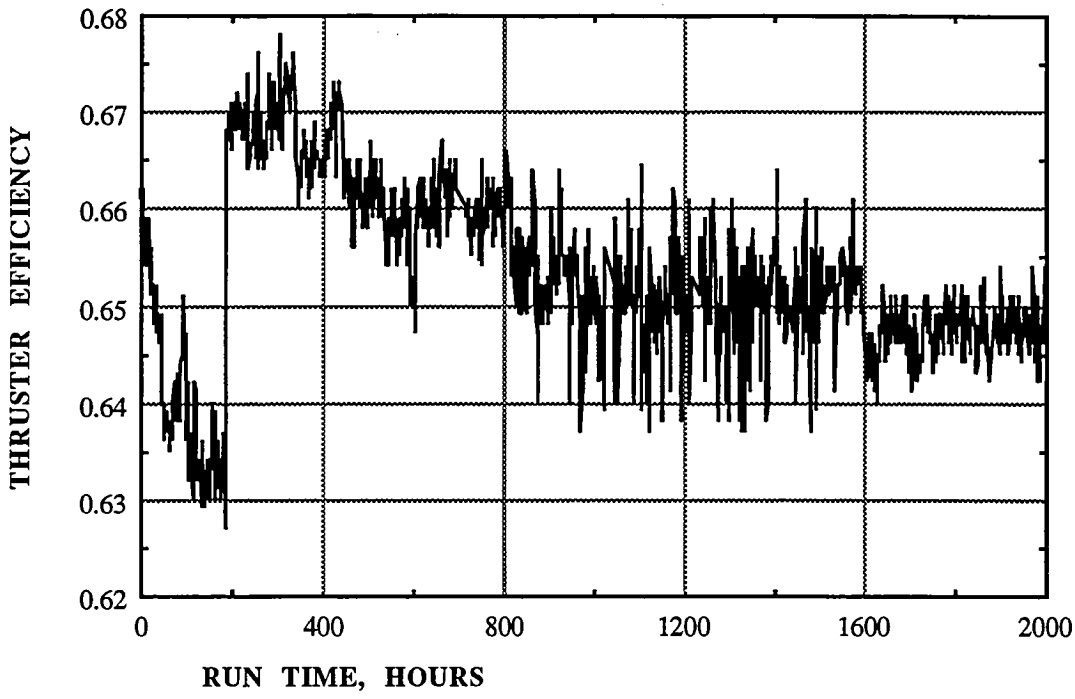

Figure 2 - Thruster efficiency versus wear test duration.

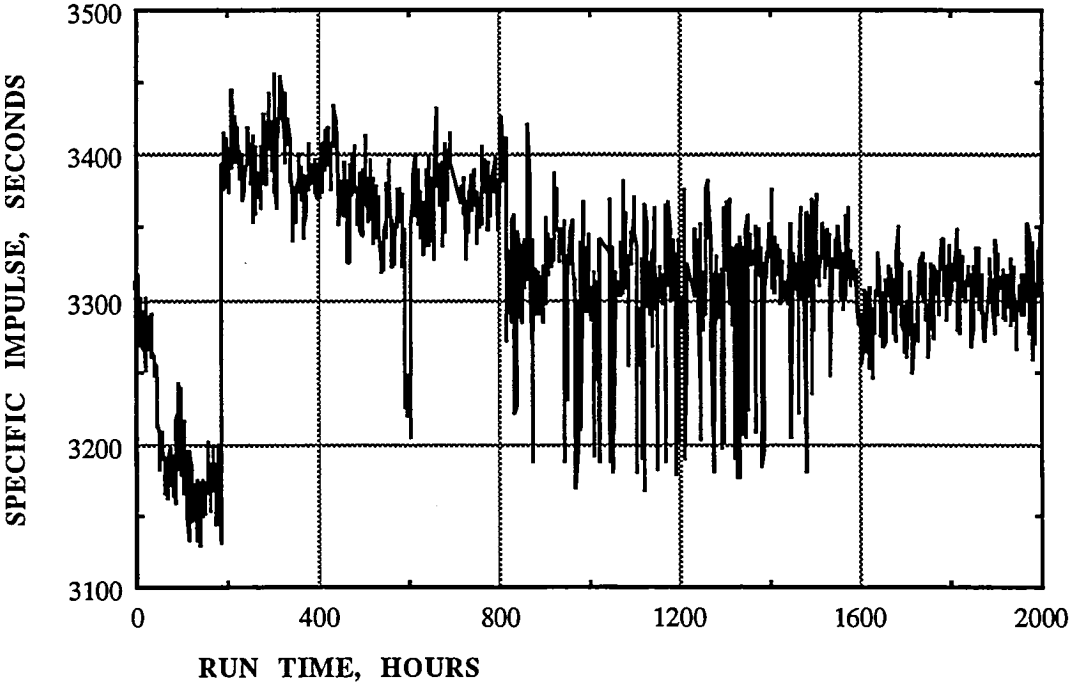

Figure 3 - Specific impulse versus wear test duration.

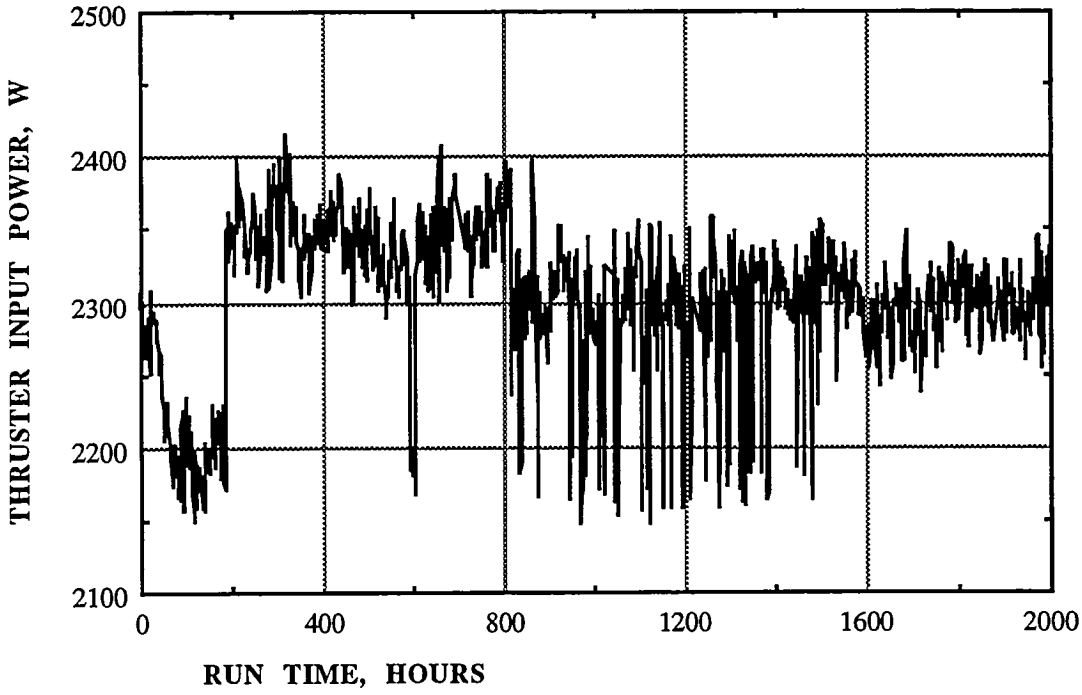

Figure 4 - Thruster input power versus wear test duration.

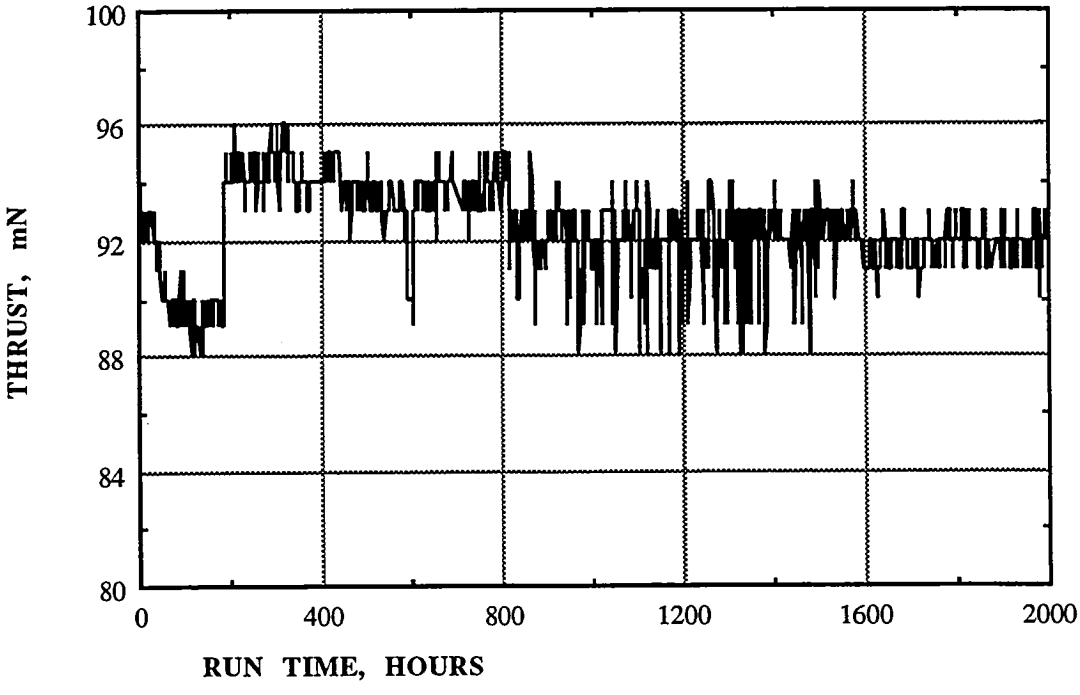

Figure 5 - Thrust versus wear test duration.

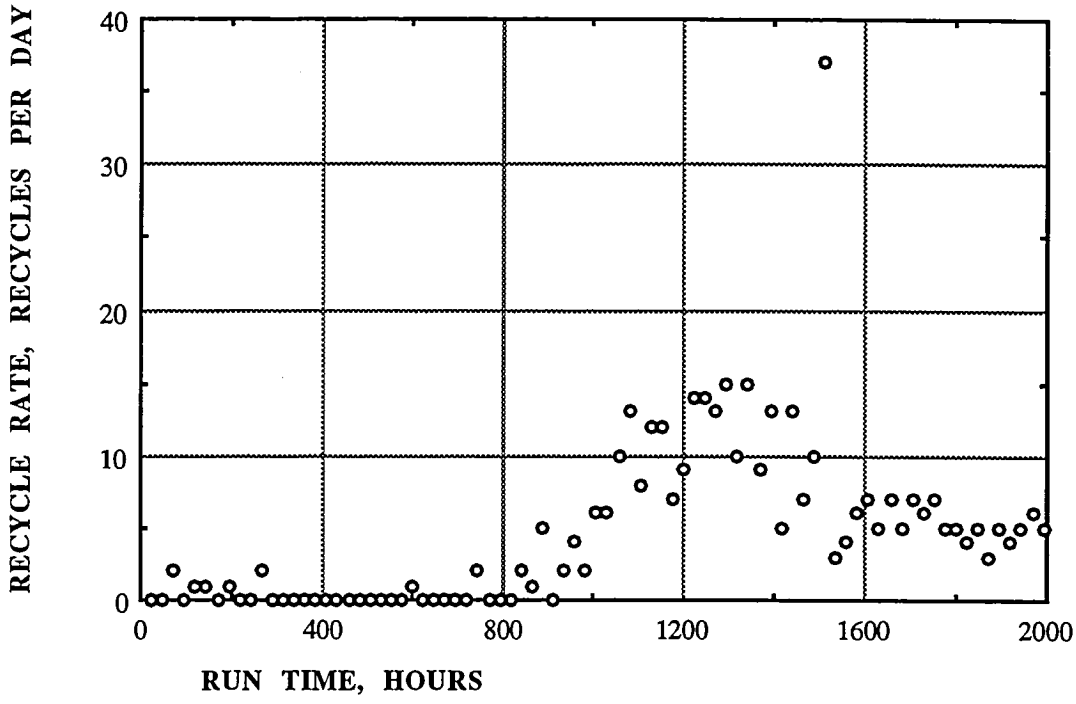

Figure 6 - Recycle frequency versus wear test duration.

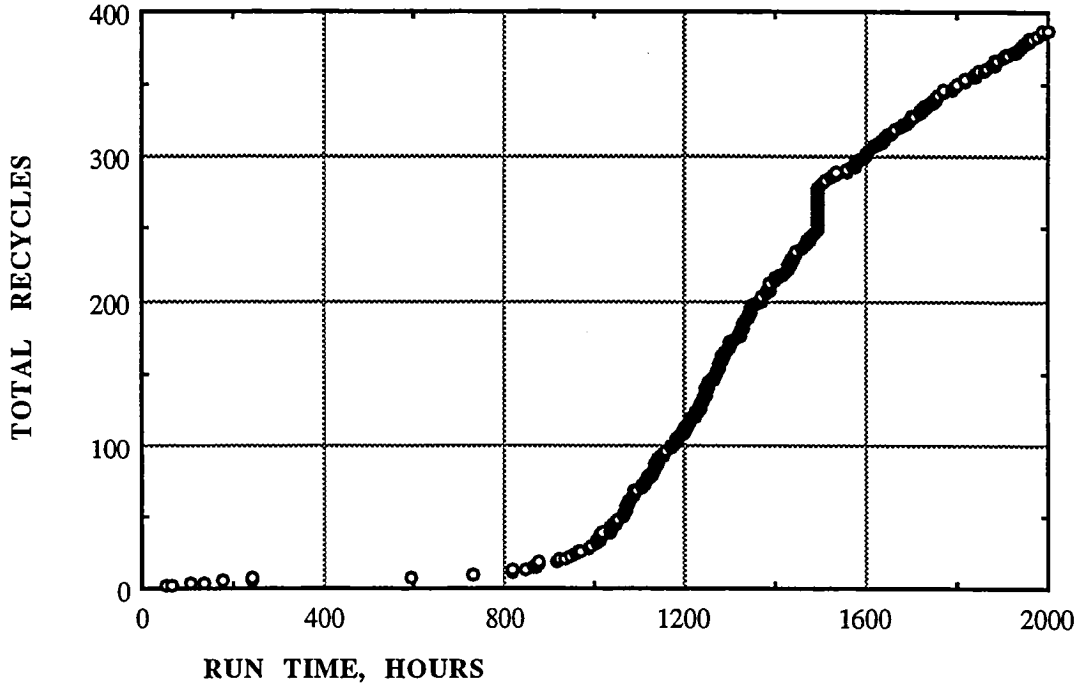

Figure 7 - Cumulative recycles versus wear test duration.

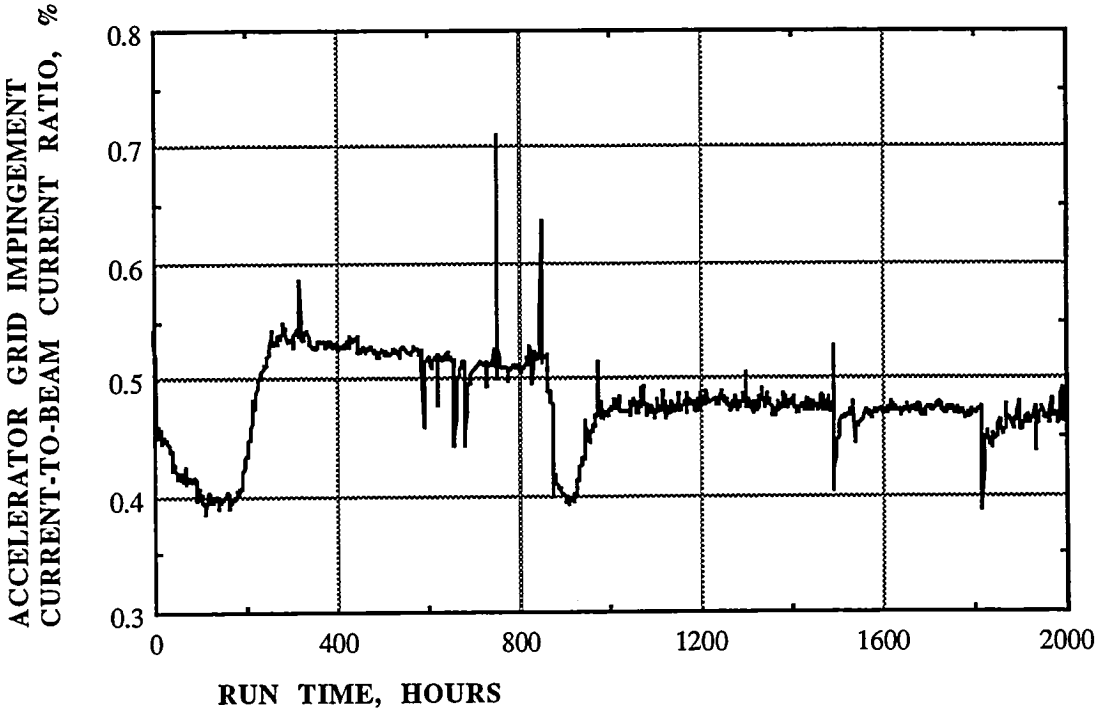

Figure 8 - Ratio of accelerator current to beam current versus wear test duration.

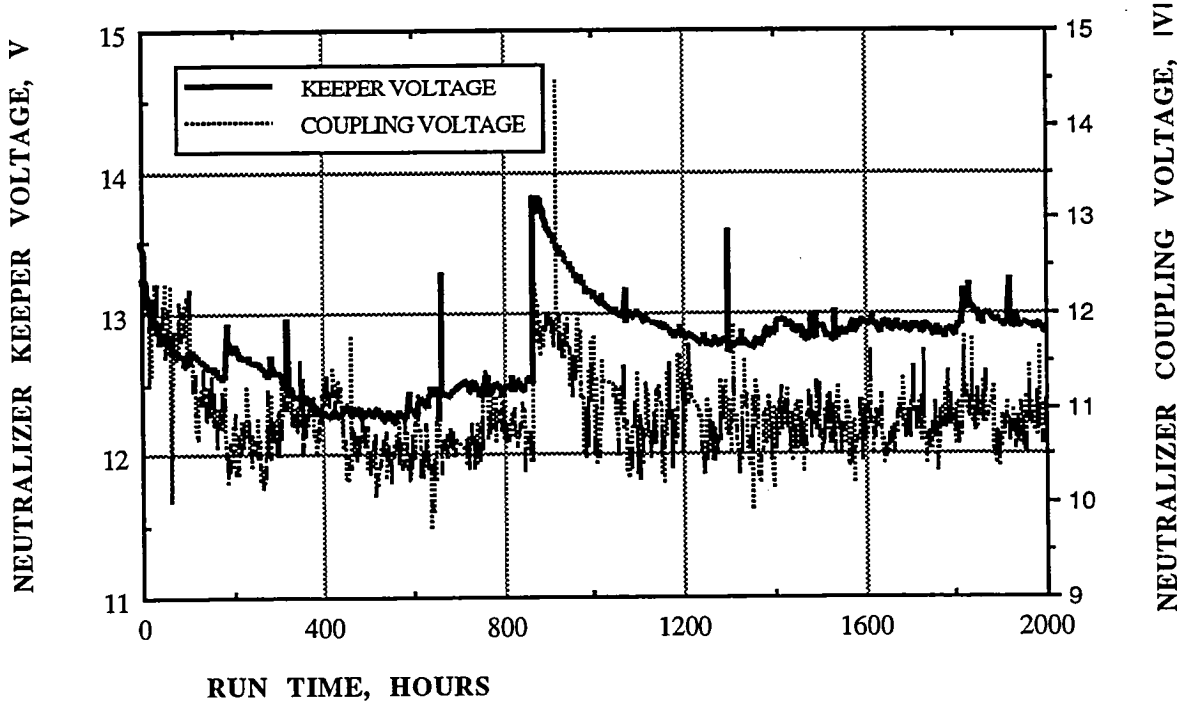

Figure 9 - Neutralizer voltages versus wear test duration.

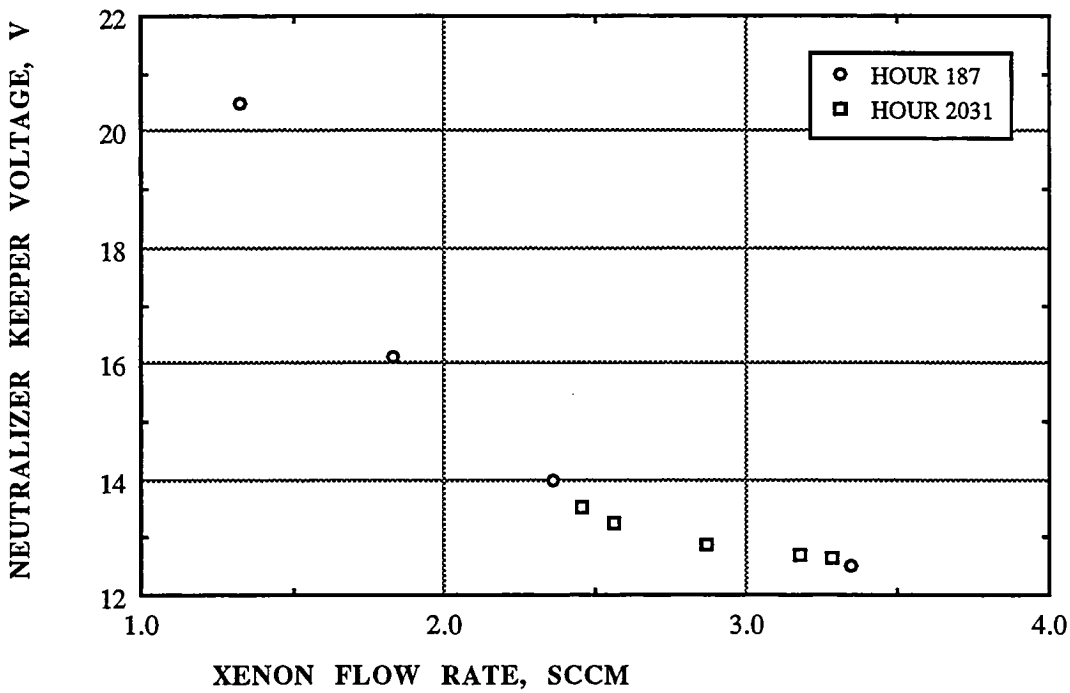

Figure 10 - Neutralizer keeper voltage versus xenon flow rate; hour 187 and hour 2031.

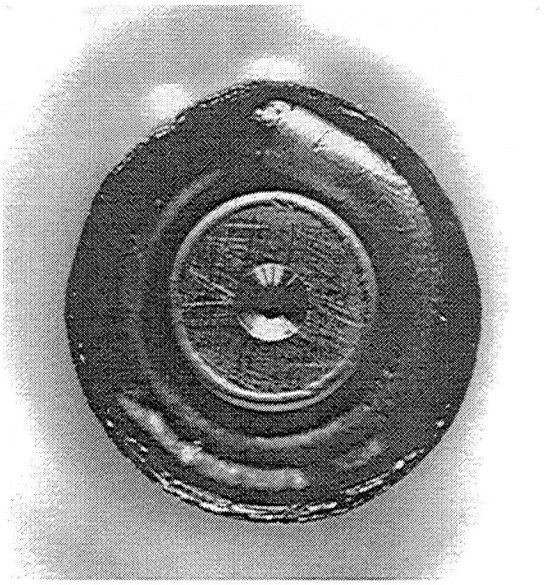

Figure 11a - Pre-test photograph of first wear test discharge cathode

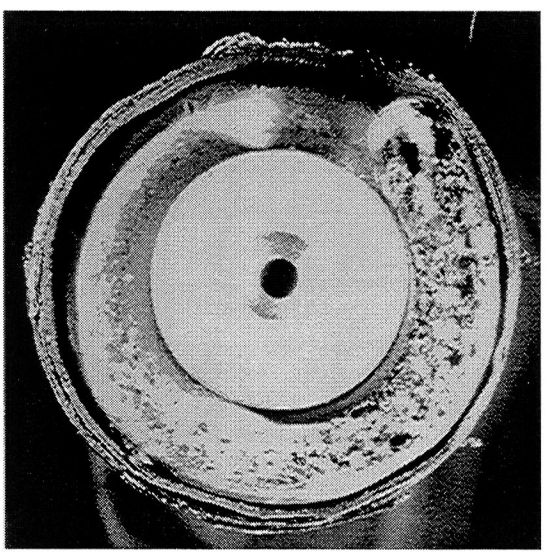

Figure 11b - Post-867 hour photograph of first wear test discharge cathode.

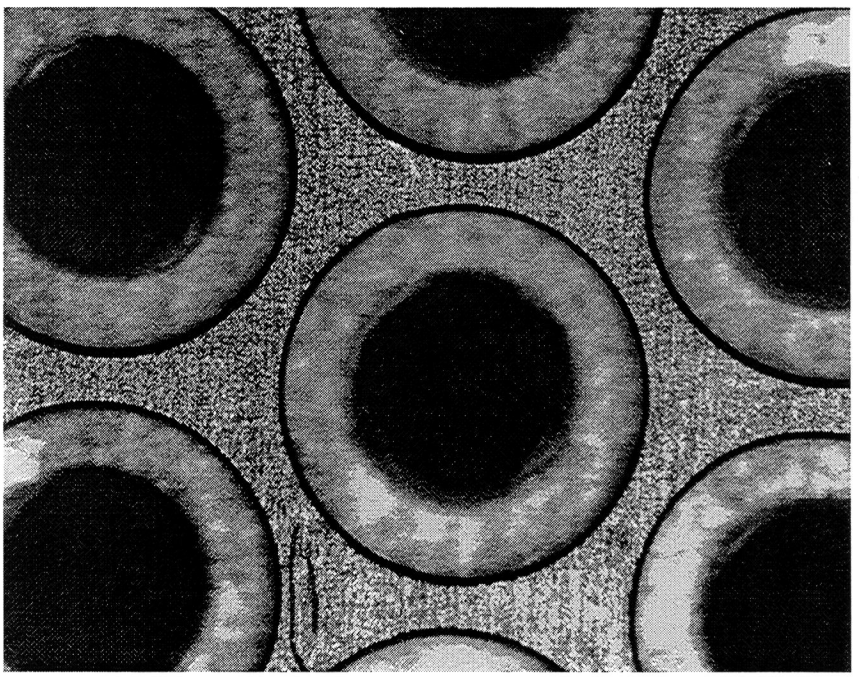

Figure 12a - Screen grid, centerline upstream, pre-test.

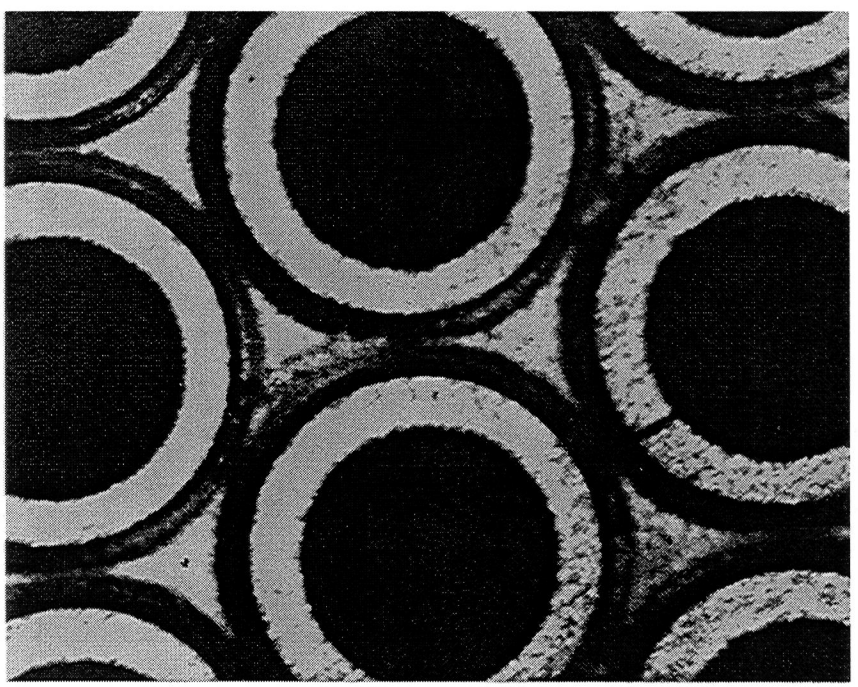

Figure 12b - Screen grid, centerline upstream, post-867 hours.

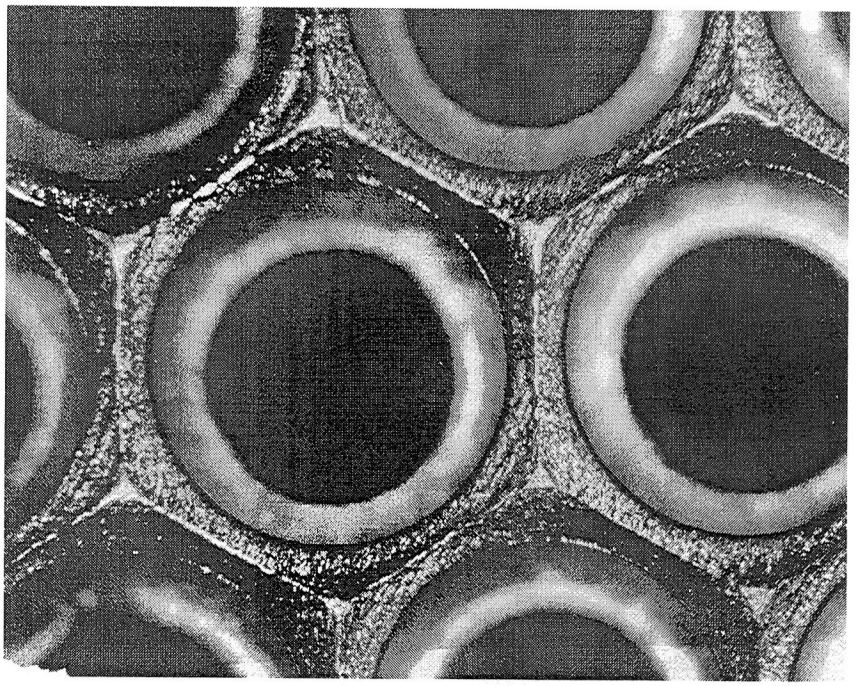

Figure 12c - Screen grid, centerline upstream, post-2150 hours.

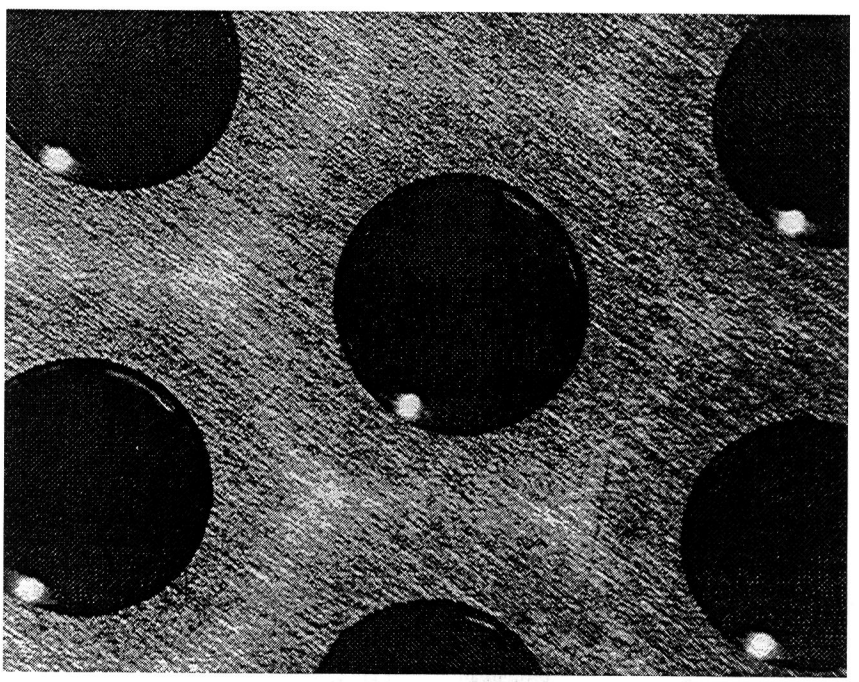

Figure 13a - Accelerator grid, centerline downstream, pre-test.

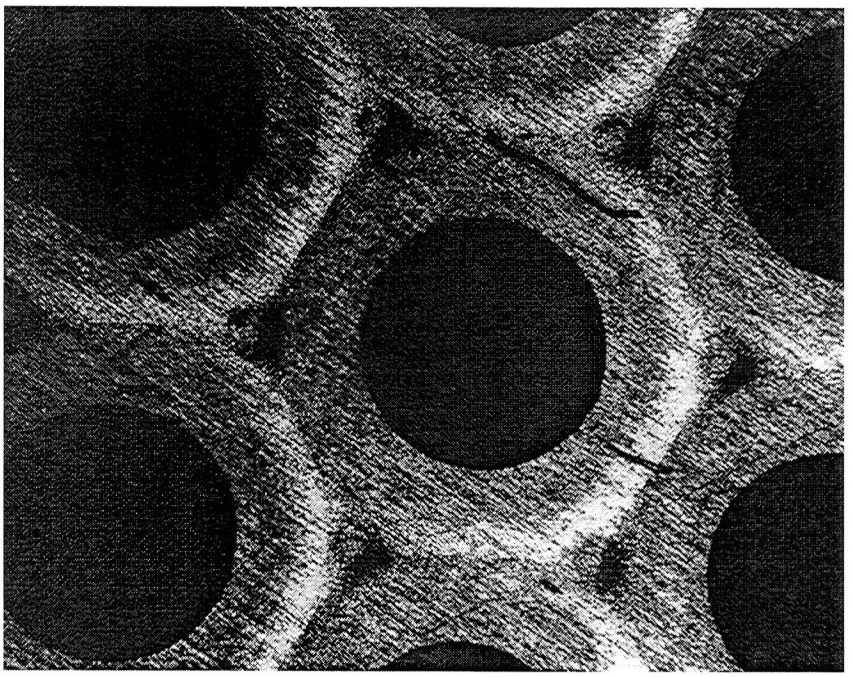

Figure 13b - Accelerator grid, centerline downstream, post-867 hours.

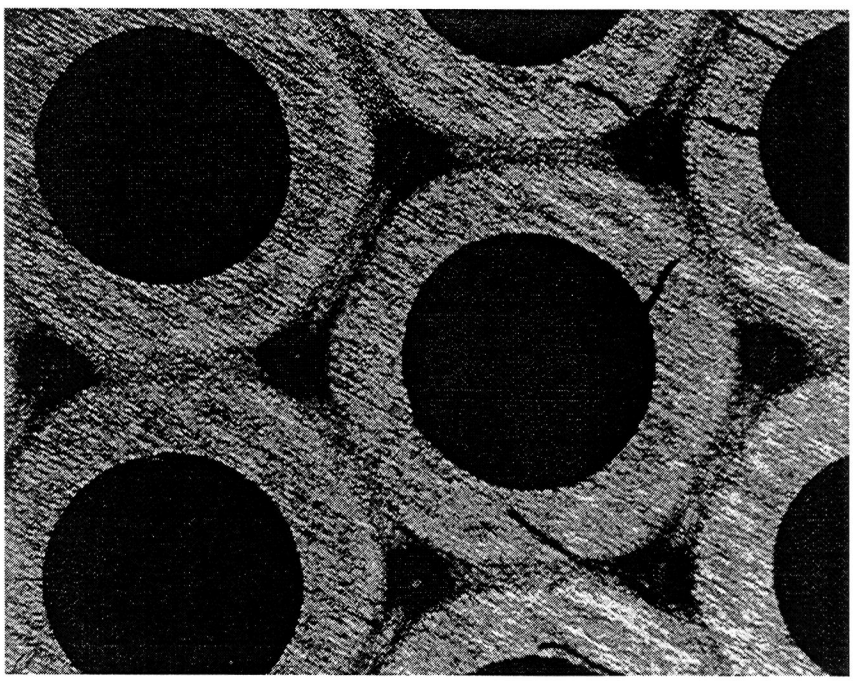

Figure 13c - Accelerator grid, centerline downstream, post-2150 hours.

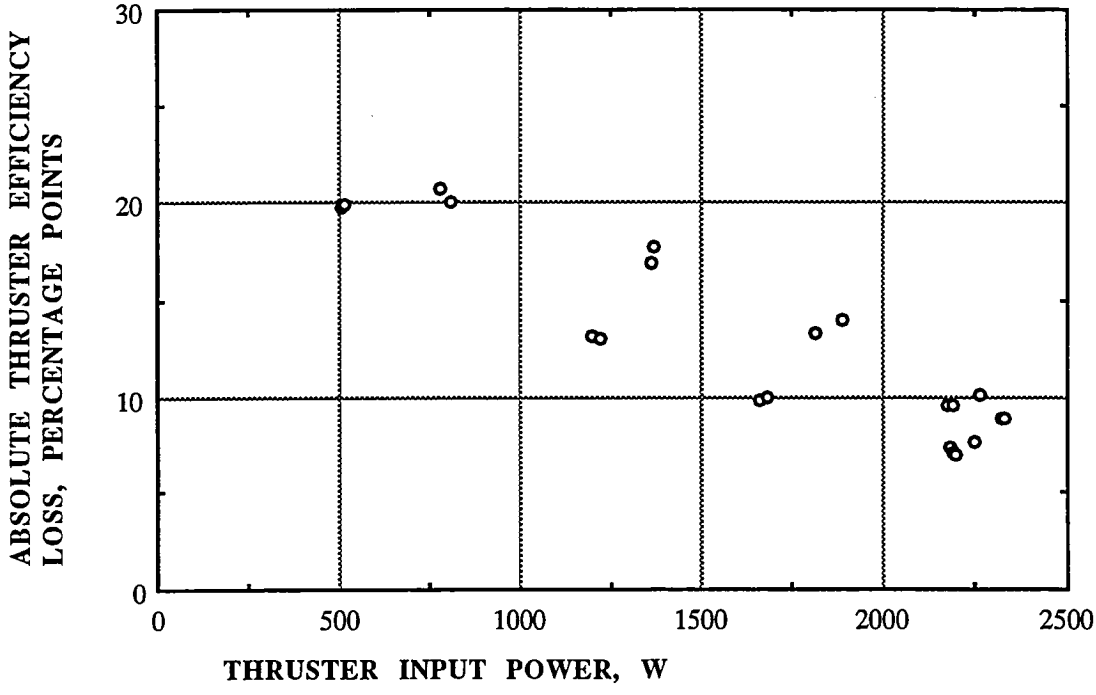

Figure 14 - Thruster efficiency loss due to neutralizer operation, versus thruster input power.

REPORT DOCUMENTATION PAGE

Form Approved
OMB No. 0704-0188

1. AGENCY USE ONLY (*Leave blank*)	2. REPORT DATE	3. REPORT TYPE AND DATES COVERED
	November 1995	Technical Memorandum

4. TITLE AND SUBTITLE

2.3 kW Ion Thruster Wear Test

5. FUNDING NUMBERS

WU-242-70-01

6. AUTHOR(S)

Michael J. Patterson, Vincent K. Rawlin, James S. Sovey,
Michael J. Kussmaul and James Parkes

7. PERFORMING ORGANIZATION NAME(S) AND ADDRESS(ES)

National Aeronautics and Space Administration
Lewis Research Center
Cleveland, Ohio 44135-3191

8. PERFORMING ORGANIZATION REPORT NUMBER

E-9940

9. SPONSORING/MONITORING AGENCY NAME(S) AND ADDRESS(ES)

National Aeronautics and Space Administration
Washington, D.C. 20546-0001

10. SPONSORING/MONITORING AGENCY REPORT NUMBER

NASA TM-107076
AIAA-95-2516

11. SUPPLEMENTARY NOTES

Prepared for the 31st Joint Propulsion Conference and Exhibit cosponsored by AIAA, ASME, SAE, and ASEE, San Diego, California, July 10-12, 1995. Michael J. Patterson, Vincent K. Rawlin, and James S. Sovey, NASA Lewis Research Center; Michael J. Kussmaul and James Parkes, NYMA, Inc., 2001 Aerospace Parkway, Brook Park, Ohio 44142 (work funded by NASA Contract NAS3-27186). Responsible person, Michael J. Patterson, organization code 5330, (216) 977-7481.

12a. DISTRIBUTION/AVAILABILITY STATEMENT

Unclassified - Unlimited
Subject Category 20

This publication is available from the NASA Center for Aerospace Information, (301) 621-0390.

12b. DISTRIBUTION CODE

13. ABSTRACT (*Maximum 200 words*)

A 30-cm diameter xenon ion thruster is under development at NASA to provide an ion propulsion option for auxiliary and primary propulsion on missions of national interest. Specific efforts include thruster design optimizations, component life testing and validation, and performance characterizations. Under this program, the ion thruster will be brought to engineering model development status. This paper describes the results of a 2.3-kW 2000-hour wear test performed to identify life limiting phenomena, measure the performance and characterize the operation of the thruster, and obtain wear, erosion, and surface contamination data. These data are being using as a data base for proceeding with additional life validation tests, and to provide input to flight thruster design requirements.

14. SUBJECT TERMS	15. NUMBER OF PAGES
Ion thruster; Xenon thruster; New millennium	32
	16. PRICE CODE: A03

17. SECURITY CLASSIFICATION OF REPORT	18. SECURITY CLASSIFICATION OF THIS PAGE	19. SECURITY CLASSIFICATION OF ABSTRACT	20. LIMITATION OF ABSTRACT
Unclassified	Unclassified	Unclassified	